Body Size and Tissue-Scaling Is Regulated by Motoneuron-Derived Activinß in *Drosophila melanogaster*

Lindsay Moss-Taylor,[1,2] Ambuj Upadhyay,[2] Xueyang Pan, Myung-Jun Kim, and Michael B. O'Connor[3]
Department of Genetics, Cell Biology and Development, University of Minnesota, Minneapolis, Minnesota 55455
ORCID IDs: 0000-0001-9242-2144 (L.M.-T.); 0000-0002-8232-3721 (A.U.); 0000-0003-4453-4971 (X.P.); 0000-0002-3067-5506 (M.B.O.)

ABSTRACT Correct scaling of body and organ size is crucial for proper development, and the survival of all organisms. Perturbations in circulating hormones, including insulins and steroids, are largely responsible for changing body size in response to both genetic and environmental factors. Such perturbations typically produce adults whose organs and appendages scale proportionately with final size. The identity of additional factors that might contribute to scaling of organs and appendages with body size is unknown. Here, we report that loss-of-function mutations in *Drosophila Activinβ (Actβ)*, a member of the TGF-β superfamily, lead to the production of small larvae/pupae and undersized rare adult escapers. Morphometric measurements of escaper adult appendage size (wings and legs), as well as heads, thoraxes, and abdomens, reveal a disproportional reduction in abdominal size compared to other tissues. Similar size measurements of selected *Actβ* mutant larval tissues demonstrate that somatic muscle size is disproportionately smaller when compared to the fat body, salivary glands, prothoracic glands, imaginal discs, and brain. We also show that Actβ control of body size is dependent on canonical signaling through the transcription-factor dSmad2 and that it modulates the growth rate, but not feeding behavior, during the third-instar period. Tissue- and cell-specific knockdown, and overexpression studies, reveal that motoneuron-derived Actβ is essential for regulating proper body size and tissue scaling. These studies suggest that, unlike in vertebrates, where Myostatin and certain other Activin-like factors act as systemic negative regulators of muscle mass, in *Drosophila*, Actβ is a positive regulator of muscle mass that is directly delivered to muscles by motoneurons. We discuss the importance of these findings in coordinating proportional scaling of insect muscle mass to appendage size.

KEYWORDS Activin; body size; hormones; motoneuron; TGF-β

SOME members of the animal kingdom, including most species of fish, amphibians, lizards, turtles, and salamanders, undergo indeterminate growth and increase their biomass throughout their life span. In contrast, birds, mammals, and many insect species exhibit determinate growth whereby ideal body length and weight is fixed upon reaching sexual maturity. This process produces a more limited range of sizes that are characteristic for the species (Hariharan *et al.* 2015). In these animals, growth rate can vary during development, and is influenced by both intrinsic and extrinsic factors. For example, in humans, at the conclusion of the high-pubertal-growth period, the long bone growth plates are ossified thereby preventing additional increase in overall skeletal size (Kronenberg 2003; Shim 2015). Similar to mammals, holometabolous insects also exhibit determinate growth. In *Drosophila*, a larva increases its mass 200-fold (70% of which occurs in the last larval instar) before terminating growth at pupariation (Church and Robertson 1966). During the non-feeding pupal stage, the adult structures differentiate from larval imaginal tissue and there is no net increase in body mass. Thus, the final body size is set by the rate of larval growth and the timing of its termination.

In recent years, numerous studies have centered on elucidating the molecular mechanisms that regulate hormonal activity during larval development in holometabolous insects

doi: https://doi.org/10.1534/genetics.119.302394
Manuscript received June 4, 2019; accepted for publication September 29, 2019; published Early Online October 4, 2019.
Available freely online through the author-supported open access option.
Supplemental material available at figshare: https://doi.org/10.25386/genetics.9913937.
[1]Department of Laboratory Medicine and Pathology, University of Minnesota, Minneapolis, MN 55455.
[2]These authors contributed equally to this work.
[3]Corresponding author: Department of Genetics, Cell Biology and Development, 6-160 Jackson Hall, Church Street, Minneapolis, MN 55455. E-mail: moconnor@umn.edu

to better understand how growth rate and duration are controlled [reviewed in Rewitz *et al.* (2013), Boulan *et al.* (2015)]. In *Drosophila*, growth is largely regulated by the Insulin/IGF Signaling (IIS) and Target of Rapamycin (TOR) pathways, which are themselves regulated by different nutritional inputs. IIS is regulated by systemic sugar concentrations and TOR by circulating amino acid levels. Mutations that attenuate either pathway lead to slower growth rates resulting in diminutive animals with smaller and fewer cells [(Chen *et al.* 1996; Böhni *et al.* 1999; Oldham *et al.* 2000; Rulifson *et al.* 2002)]. Conversely, activation of either pathway can lead to larger organs and cells if there are adequate nutrients (Leevers *et al.* 1996; Goberdhan *et al.* 1999; Stocker *et al.* 2003). Interestingly, systemic manipulation of IIS/TOR pathways typically leads to smaller or larger animals, with proportional effects on organ and appendage size (allometric growth) (Shingleton *et al.* 2007; Shingleton and Frankino 2013).

While IIS/TOR are central regulators of growth rate in holometabolous insects, the major regulator of growth duration is the steroid hormone 20-hydroxyecdysone (20E) [reviewed in Yamanaka *et al.* (2013a)]. During the final larval stage, a pulse of 20E extinguishes feeding, terminates growth, and initiates pupariation. The timing of the 20E pupariation pulse is triggered, in part, by the neuropeptide prothoracicotropic hormone (PTTH), which in *Drosophila* is produced by the two pairs of neurons in each brain hemisphere that innervate the prothoracic gland (PG) (McBrayer *et al.* 2007; Shimell *et al.* 2018). PTTH binds to its receptor Torso, and stimulates the synthesis and secretion of ecdysone from the PG (Rewitz *et al.* 2009; Yamanaka *et al.* 2013a). PTTH production/release responds to a variety of environmental signals including nutritional status, light, and tissue damage, as well as internal signals such as juvenile hormone (JH), to further tune the timing of pupariation (Yamanaka *et al.* 2013b; De Loof *et al.* 2015; Shimell *et al.* 2018).

In addition to IIS/TOR signaling and steroid hormones, other signaling pathways have also been identified that affect final body mass and proportion scaling in both vertebrates and invertebrates. In particular, the TGF-β signaling pathway has known roles in controlling cell, tissue, and body size. TGF-β superfamily ligands signal by binding to a heterotetrameric complex of type I and type II serine–threonine receptor kinases. Ligand binding triggers type II receptors to phosphorylate type I receptors, thereby activating their kinases (Heldin and Moustakas 2016). In canonical signaling, the activated type I receptor phosphorylates its major substrates, the receptor-smad (R-Smad) [reviewed in Hata and Chen (2016)]. Once phosphorylated, R-Smads oligomerize with co-Smads and translocate to the nucleus where, together with other cofactors, they regulate gene transcription [review in Hill (2016)]. The ligand superfamily is broadly divided into two major subdivisions based on phylogenetic and signaling analysis (Kahlem and Newfeld 2009). These include the TGF-β/Activins, which in vertebrates signal through R-Smads 2/3, while the bone morphogenetic protein (BMP)/growth and differentiation factor (GDF)-type factors signal through R-Smads 1/5/8 (Macias *et al.* 2015).

TGF-β family members contribute to tissue and body size growth by a variety of mechanisms. For instance, in mammalian mammary cells, TGF-β cell-autonomously regulates cell size via mTOR during epithelial–mesenchymal transition (Lamouille and Derynck 2007). In addition, BMPs have been shown to control cell proliferation at the long bone growth plate and have been identified by genome-wide association studies as regulating human height (Hirschhorn and Lettre 2009; Wood *et al.* 2014). Another particularly stunning example is Myostatin, a circulating Activin-type ligand, whose loss causes skeletal and muscle hypertrophy in vertebrates (McPherron and Lee 1997; McPherron *et al.* 1997). TGF-β-type factors also affect the body size of invertebrates. For example, in *Caenorhabditis elegans*, a BMP-type ligand, *DBL-1*, is secreted from neurons and signals via *small* (*sma*), a worm Smad, in the hypodermis to regulate expression of cuticle genes (Tuck 2014; Madaan *et al.* 2018). In *Drosophila*, the BMP family member Dpp has a well-characterized role in regulating imaginal disc growth, but it has not been shown to influence overall larval body size (Upadhyay *et al.*, 2017).

To further explore how different TGF-β ligands influence body size, we investigated the role of *Drosophila* Activinβ (Actβ) in regulating these traits using both loss- and gain-of-function studies. In *Drosophila*, genetic studies as well as phylogenetic analysis suggest that Actβ signals via Baboon (Babo) and Punt, type I and type II receptors, respectively, to phosphorylate dSmad2 [reviewed in Upadhyay *et al.* (2017)]. We find that canonical Actβ signaling through dSmad2 regulates adult viability, body size, and tissue scaling. *Actβ* mutants produce small larvae and pupae along with rare adult escapers. Compared to controls, these rare mutant adults exhibit small abdomens while other structures, such as the head, thorax, leg, and wing, are of relatively normal size. In larvae, muscle size is most profoundly affected while imaginal discs and the larval brain are of normal size. Furthermore, *Actβ* mutants have a slower overall growth rate, but show no defects in food intake. Using tissue-specific gain- and loss-of-function, we demonstrate that motoneuron-derived Actβ is required for proper muscle growth and adult viability. Conversely, hyperactivation of Activin signaling in muscles by overexpression of activated Babo produces a much larger animal with bigger muscles, but smaller imaginal discs. These observations demonstrate that muscle size can be perturbed without having proportional effects on the size of the imaginal tissues. Therefore, we suggest that coordination of muscle and appendage growth requires *Actβ* signaling, but that other environmental factors, perhaps including nutrition and temperature, are also likely involved.

Materials and Methods

Fly lines

For overexpression experiments, single copies of Gal4 and upstream activating sequence (UAS) transgenes were used.

Actβ-Gal4 and *UAS-Actβ* (3B2) were previously described (Zhu *et al.* 2008). *C929-Gal4*, dilp2-*Gal4*, *Elav-Gal4*, *Mef2-Gal4*, *MHC-Gal4*, *Nrv2-Gal4*, *OK371-Gal4*, *ppl-Gal4*, *UAS-dicer2*, *UAS-cd8::GFP*, and *UAS-Actβ RNAi* (RNA interference) *Ok6 > Gal4* were all from the Bloomington *Drosophila* Stock Center (BDSC). *UAS-babo RNAi* and *UAS-dSmad2 RNAi* were from O'Connor laboratory stocks (details of construction available upon request). *UAS-dSmad2^{SDVD}* and UAS-babo* (constitutively activated) was previously described (brummell 1999 Gesualdi and Haerry 2007).

The *Actβ^{80}* allele is an EMS-induced substitution leading to a premature stop codon and presumed to be a null mutation (Zhu *et al.* 2008). The chromosome carrying the *Actβ^{80}* allele (fourth) also contains a variegating w^+ transgene (P{hsp26-pt-T}39C-12, FlyBase identifier = FBti0016154) inserted between *Hcf* and *PMCA*. This w^+ transgene causes red speckles with dominant inheritance in an otherwise w^- background.

Actβ^{4E}, *Actβ^{10E}*, and *Actβ^{4dd}* were all generated using the clustered regularly interspaced short palindromic repeats (CRISPR)/Cas9 system. Two guide RNAs were cloned into the *Bbs*I site of the pU6-BbsI-chiRNA plasmid (obtained from Addgene) and injected by Best Gene into *w^{1118}*; *PBac{y[+mDint2]=vas-Cas9}VK00027* on chromosome 3 (#51324; BDSC). The following guides were used to target the genomic locus: guide 1, 5′-GGGTTGTGGAAATGACTTCC-3′ and guide 2: 5′-GCGATT GCACGGGCTCTTTT-3′. G0 male flies were backcrossed to a balancer stock (*CiD/unc13-GFP*) to isolate *w^{1118};;;Actβ$^{?}$/unc-13-GFP* stocks. To identify new *Actβ* alleles, DNA from homozygous (non-GFP) larvae was used to PCR amplify the genomic region flanking the CRISPR target sites using the following primers (FWD: 5′-CTGCTGCAACAGCCTTGGCTCCC-3′; REV: 5′-GGGGCGCAACACGGTCGCATTCC-3′).

Line 4E and 4dd are independent ∼3-kb deletions that remove exons 2 and 3. Line 10E is a ∼1.3-kb deletion that removes exon 4 and 5. Exact deletion junction sites are available upon request.

Rearing conditions

Eggs were collected over a 2–3-hr time period on apple juice plates inoculated with yeast paste and aged until hatching into first-instar larvae. Larvae of the desired type were then transferred to vials containing standard cornmeal food (Bloomington recipe) or 5% sucrose, 5% yeast, and 1% agar (w/v) (Figure 1, Figure 2, Figure 3, Figure 5, Figure 7, Figure 8, and Supplemental Material, Figures S1 and S5), and incubated at 25° in a 12-hr light/dark cycle until scoring. Animals were transferred to vials at a low density (30 or 40 per vial) to prevent crowding affects.

Size measurements of larval tissues and nuclei

To measure the sizes of larval organs, tissues were prepared using standard protocols for immunohistochemistry (see below). To measure the sizes of larval body-wall muscles, larval fillets of late wandering L3 larvae were prepared, and the surface area of muscle #6 of the A2 segment was measured in FIJI by outlining the muscle segment using the free-hand selection tool. Larval brains were stained with DAPI and rhodamine-phalloidin, and placed onto a glass microscope slide between two #2 coverslips that acted as a bridge to prevent deforming the shape of the brain lobes. Confocal Z-stacks of the entire lobe were captured, and manual 3D segmentation using ITK-SNAP (PMID: 16545965) was used to measure lobe volume. Imaginal discs were stained with DAPI, imaged using confocal microscopy, and then maximum-intensity projections were generated and processed in FIJI, using the threshold and measure functions to obtain a two-dimensional (2D) area of each disc. For the fat body, proventriculus, and muscle salivary glands and the PG, tissue was stained with DAPI and rhodamine-phalloidin, and then Z stacks obtained. Nuclear size was measured using FIJI (Schindelin *et al.* 2012) at the sections where nuclei were largest.

Pupal volume determination

Pupal volume was calculated from the length and width of individual pupae assuming a prolate spheroid shape [$V = (4/3)\ \pi\ (\text{width}/2)^2\ (\text{length}/2)$] (Demontis and Perrimon 2009). Pupal length was measured from the anterior tip midway between spiracles to the base of the posterior spiracles. Pupal width was measured at the widest point of the pupae.

Measurement of adult appendage sizes

Adult specimens were fixed in 95% ethanol. Structures were dissected and mounted in Canadian Balsam (C1795; Sigma [Sigma Chemical], St. Louis, MO) and Wintergreen oil (M2047; Sigma) solution (50:50). To measure size (length or area) of adult body parts, images were processed in FIJI using either the free-hand or polygon tool (illustrated by red lines in Figure 2).

Developmental timing and growth assay

To measure developmental timing, flies were transferred to a constant light environment for at least 2 days prior to egg lay and all subsequent assays were carried out under constant light conditions to avoid circadian rhythms. Eggs were collected on apple juice plates with yeast paste for 2–5 hr. The next day, early L1 larvae were transferred to standard cornmeal food with yeast paste and an additional synchronization step was employed at L2/L3 ecdysis. For developmental timing assay, 20–30 synchronized L2–L3 ecdysing larvae were transferred to cornmeal food without yeast paste to measure time to pupariation. Pupariation was scored every 2 hr by monitoring for anterior spiracle eversion and larval movement. The half point is the time it takes for one-half of the population to pupariate, which is calculated using a simple linear regression.

To measure growth rate, L3 larvae were cultured for appropriate times after L2–L3 ecdysis, washed in water, and weighed individually on a Mettler Toledo XP26 microbalance. For adult mass, groups of 8–10 animals were weighed on the microbalance.

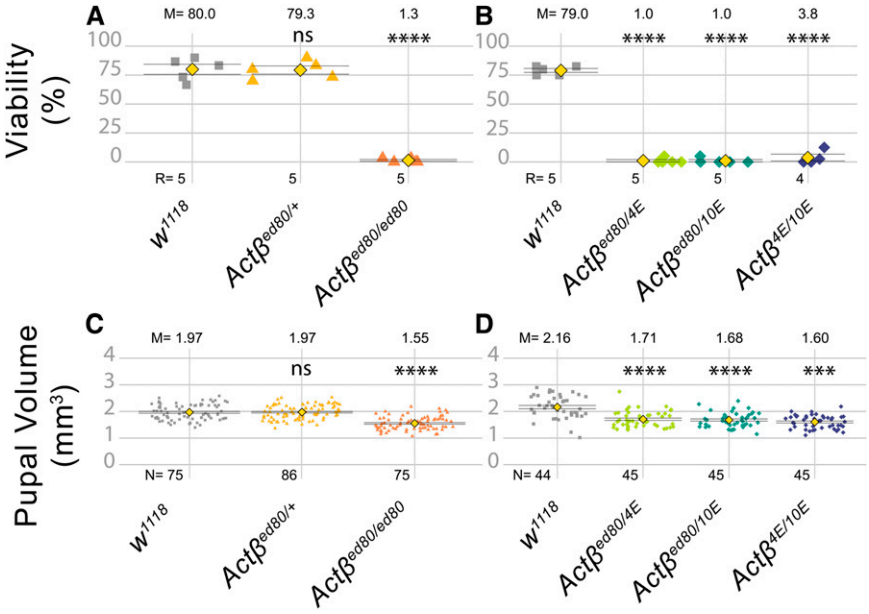

Figure 1 *Actβ* null mutants exhibit a small body size and late pupal lethality. (A and B) Most *Actβ* mutants die as late pharates in the pupal case, with between a 1–4% escaper rate. Heterozygotes and w^{1118} controls exhibit ~80% viability. (C) Pupal volume of $Actβ^{80}$ (mixed male and female pupae) null mutants (orange triangles, 1.55 mm^3) are ~20% smaller than heterozygous individuals (yellow triangle, 1.97 mm^3) and w^{1118} controls (gray squares, 1.97mm^3) (D) Pupal volumes of other *Actβ trans*-heterozygous mutant combinations show similar decreases in pupal volume. M is the sample mean shown above each data set, N is the sample size for pupal volume, and R is number of replicates for each genotype (A and B); each replicate consists of 30–40 larvae. Means indicated by yellow diamond ± SEM. **** $P < 0.0001$. ns, not significant.

Statistics

Data were analyzed using either GraphPad Prism or R-studio. A single test variable was compared to a single control using Welch's two-sample *t*-test. Multiple test variables were compared to controls using a one-way ANOVA followed by Tukey's multiple comparison test. For rescue experiments with two controls and one test cross, the test cross must be significantly different in the same direction (*e.g.*, larger) to be considered a significant result. Where the test cross was reported to be *x* units different from the controls, the different was in reference to the control with smaller variation. *P*-value designations were: ns = not significant, * $P < 0.05$, ** $P < 0.01$, *** $P < 0.001$, and **** $P < 0.0001$.

Immunohistochemistry

Wandering third-instar larvae were rinsed, dissected, fixed in 3.7% formaldehyde in PBS for 25 min, and then washed three times in PBS (0.1%)-Triton X-100. Samples were incubated with primary antibody overnight at 4° followed by secondary antibodies for 2 hr at 25°. Tissues were mounted in 80% glycerol. The following stains and antibodies were used: rhodamine-phalloidin (R415; Molecular Probes, Eugene, OR), α-Dachshund (mAbdac2-3; DSHB), α-PTTH (guinea pig, a gift from P. Leopold), α-p-Mad (Eptitomics), and α-DIMM (a gift from P. Taggert).

Microscopy

Confocal images were generated using a Zeiss ([Carl Zeiss], Thornwood, NY) Axiovert microscope with a CARV attachment or Zeiss LSM710. Pupae, adult heads, and bodies were imaged live with a Zeiss Stemi stereo microscope using a 1× objective. Adult wings and legs were imaged using a Nikon (Garden City, NY) Optiphot light microscope with a 4× objective. Trichomes were imaged using a 40× objective.

Western blots

L3 larvae were dissected and all organs were removed from the carcass samples. Carcass samples were lysed with reducing gel loading buffer. Bands were resolved on 4–12% gradient gels (Invitrogen, Carlsbad, CA) and transferred to a PVDF membrane (Bio-Rad, Hercules, CA). Membrane blocking and antibody incubation were performed using standard protocols for ECL detection. α-pSmad2 (CST, 138D4) and α-tubulin (T9026; Sigma) were used at 1/1000 dilutions. Bands were visualized using Pierce ECL Western Blotting Substrate (#32209).

Data availability

The source code for generating Figure 1, Figure 5, Figure 7, Figure 8, and Figure S1 is available at the following GitHub link: https://github.com/lindsaymosstaylor/umn-oconnorlab-activinbeta.

Strains and plasmids are available upon request. Movie S1 illustrates the defective shock response of Actβ escaper females compared to heterozygous controls. Movie S2 shows a close-up view of Actβ mutant females exhibiting poor locomotion and a held-out wing phenotype compared to heterozygous controls. Movie S3 demonstrates a defective shock response of adults in which Actβ was knocked down in motoneurons using RNAi (Ok371 > Gal4, UAS Actβ RNAi). Movie S4 shows a close up view of Ok371 > Gal4, UAS Actβ RNAi Actβ knockdown adults exhibiting poor locomotion and a held-out wing phenotype similar to that exhibited by Actβ null escaper flies (Movie S1). Supplemental material available at figshare: https://doi.org/10.25386/genetics.9913937.

Results

Actβ is required for adult viability, normal body size, and correct tissue scaling

Drosophila Actβ has been shown to be involved in a diverse group of developmental processes, including neuroblast

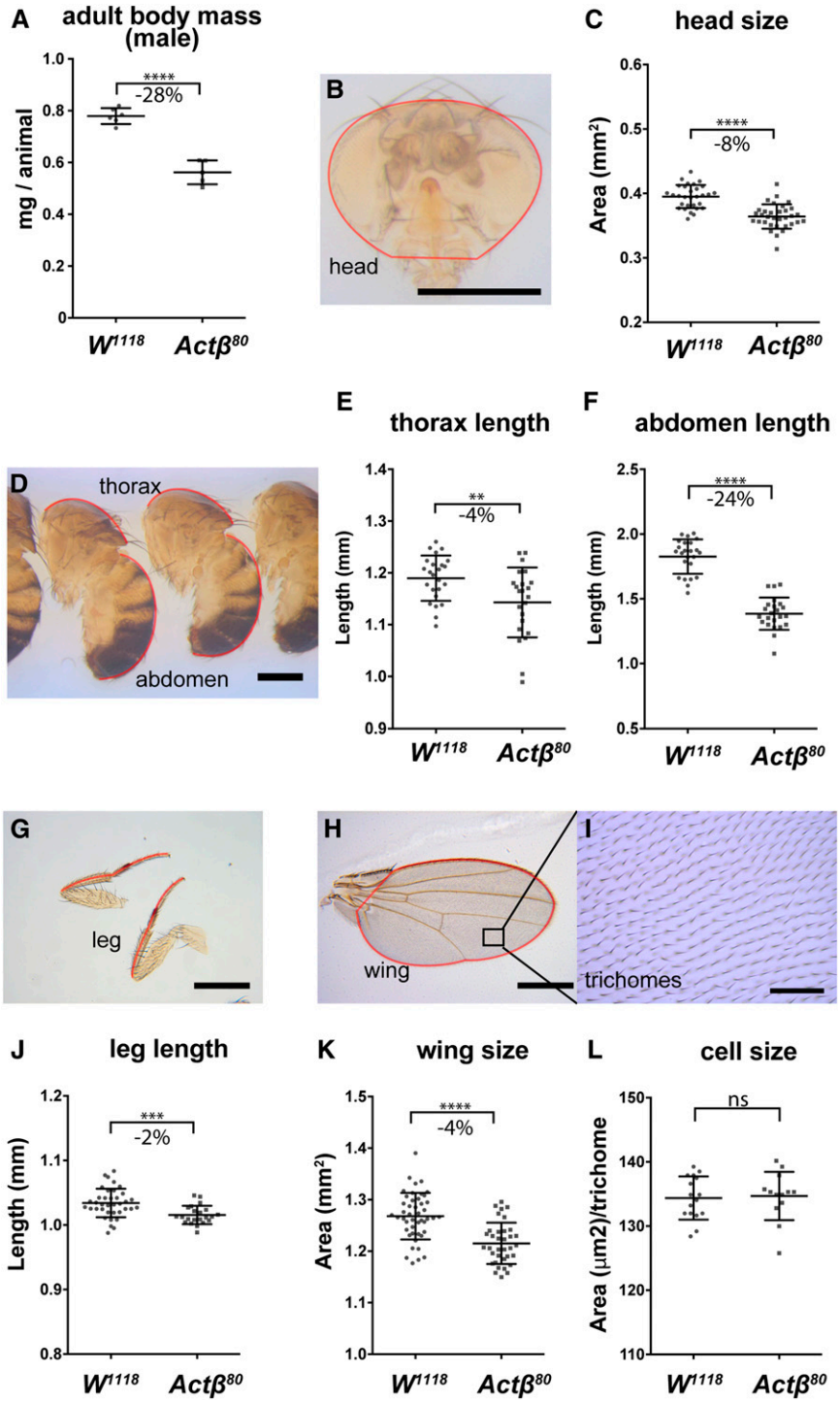

Figure 2 *Actβ* mutant adult escapers have a disproportionately smaller abdomen compared to head, thorax, leg, or wing. (A) $Act\beta^{80}$ mutant males that eclose as adults weigh ~28% less than *vs.* w^{1118} controls (n = 3–4 groups containing 9–10 individuals). (B and C) Heads of mutant males are ~8% smaller (Bar, 500 μm; $n > 30$). (D-F) Thorax (D and E) and abdomens (D and F) are ~4% and ~24% smaller, respectively (Bar, 500 μm; n = 23). (G and J) Legs and wings (H and K) of mutants are ~2% and ~4% smaller, respectively (Bar, 500 μm; n = 22–46). (I and L) Trichome density in the adult wing shows no difference in cell size (Bar, 50 μm; n = 13–16). Means ± SD are shown. All body part images are of Act^{80} mutant male flies and the red outline indicates the portion of the appendage that was measured. ** $P < 0.01$, *** $P < 0.001$, and **** $P < 0.0001$. ns, not significant.

proliferation, photoreceptor tiling, regulation of Akh signaling, and interorgan regulation of mitochondrial and hemocyte function (Ting *et al.* 2007; Zhu *et al.* 2008; Makhijani *et al.* 2017; Song *et al.* 2017a,b). However, in none of these studies was the lethal stage or the gross morphological phenotype carefully documented. To examine this issue, we initially characterized mutant phenotypes using the previously reported putative $Act\beta^{80}$ null allele (nonsense mutation) (Zhu *et al.* 2008). However, since the *Actβ* locus is on the fourth chromosome, additional recessive background mutations on the $Act\beta^{80}$ chromosome cannot be removed by recombination and therefore could complicate the phenotypic analysis of homozygous $Act\beta^{80}$ mutants. To resolve this issue, we generated several independent deletion alleles ($Act\beta^{4E}$, $Act\beta^{10E}$, and $Act\beta^{4dd}$) in the w^{1118} background using the CRISPR/Cas9 system (Ren *et al.* 2013; Sebo *et al.* 2014). All phenotypes initially described using Act^{80} homozygotes were confirmed using different combinations of

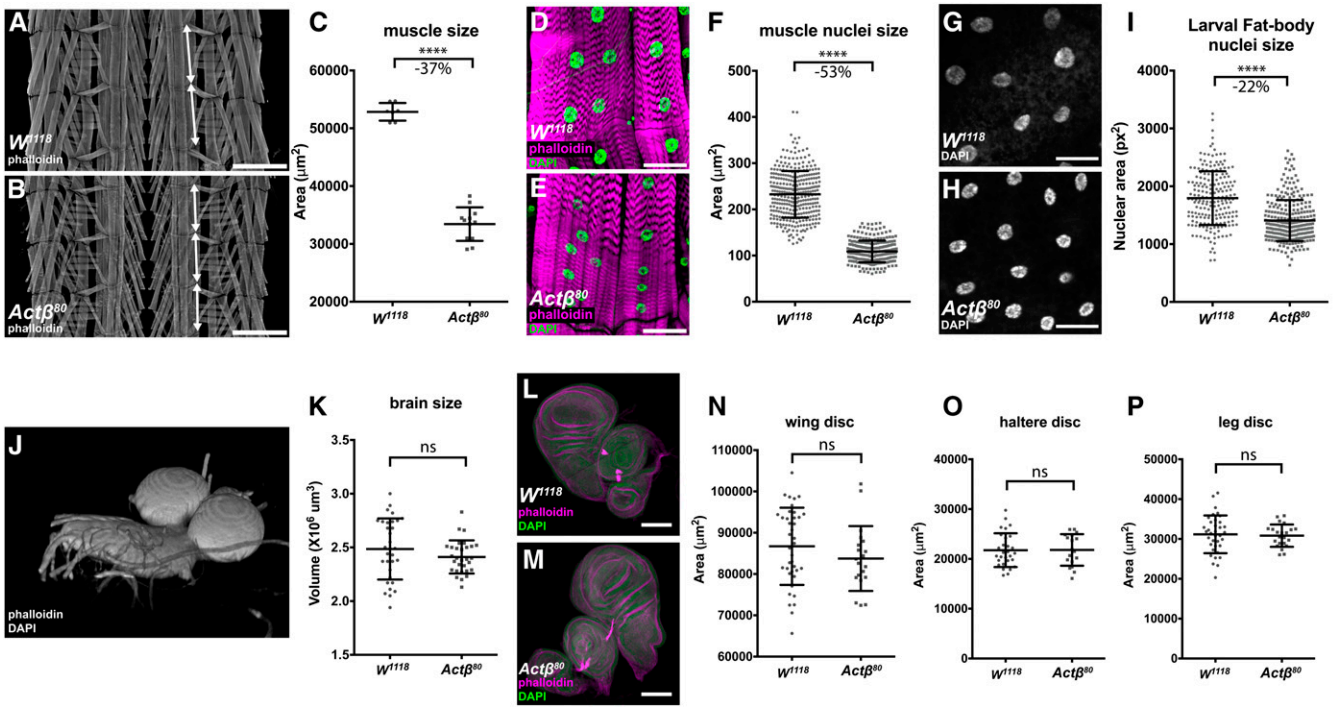

Figure 3 Actβ disproportionately affects larval body-wall muscle and fat body nuclei sizes. Late-wandering male L3 larvae were dissected and the sizes of various tissues determined. (A and B) Larval fillets were stained with rhodamine-phalloidin and imaged in the muscle plane. Double-headed arrows mark the extent of a larval segment photographed at the same magnification (Bar, 500 μm). Note that around three segments of *Actβ* mutant muscles occupy the same area as two wild-type segments. (C) Loss of *Actβ* results in a 37% decrease in the surface area of muscle #6 from the A2 segment compared to control (n = 7–12). (D–F) Muscle nuclei (DAPI, green) of *Actβ* mutants are 53% smaller (Bar, 50 μm; $n > 250$) than controls. (G–I) Fat body nuclei (DAPI, gray) of *Actβ* mutants are 22% smaller than control (Bar, 50 μm, $n > 200$). (J and K) Three-dimensional reconstruction of larval brains stained with DAPI and rhodamine-phalloidin, the volume of each brain lobe was measured separately and *Actβ* mutants showed no significant differences of brain size compared to control ($n > 30$). (L–P) Wing, leg, and haltere imaginal discs (DAPI green, phalloidin magenta) of *Actβ* mutants are the same sizes as controls. Bar, 100 μm ($n > 20$ in each group). Means ± SD are shown. **** $P < 0.0001$. ns, not significant.

transheterozygous alleles to rule out fourth chromosome background effects.

All examined *Actβ* mutant alleles are predominantly late pupal (pharate)-stage lethal (Figure 1, A and B). Sexing the pupae revealed that equal numbers of males and females made it to the pharate stage (N counted =157, male = 76, female =81). Many of the pharates showed limited movement inside the pupal case, but most never eclosed. Manual cracking of the operculum allowed a small percentage (~1%) to escape and produce viable adults in a 2:1 male/female ratio that exhibited severe locomotive defects, and held-out immobile wings rendering them flightless (Movies S1 and S2). Despite these behavioral/physical defects, females could mate and produce offspring from wild-type males. *Actβ* mutant males were unable to produce progeny with either mutant females or wild-type females. Whether this is a behavioral issue (*i.e.*, unable to initiate courtship behavior) or a fertility defect was not determined.

In addition to pharate lethality, *Actβ* mutants exhibit a small body size at all stages of development. $Act\beta^{80}$ homozygous pupae (mixed male and female populations) are 21% smaller by volume relative to w^{1118} or heterozygous pupae (Figure 1C). Similar to the $Act\beta^{80}$ homozygous phenotype, all *trans*-heterozygous combinations ($Act\beta^{80/4E}$, $Act\beta^{10E/80}$, and $Act\beta^{10E/4E}$) are also significantly smaller (21, 22, and 26%, respectively) compared to the w^{1118} control (Figure 1D), indicating that the small pupal size is not caused by secondary mutations on the mutant chromosome. Taken together, these data indicate that *Actβ* is required to produce normal pupal volume and adult viability.

Appendage size is proportionally scaled with body mass in *Drosophila* (Mirth and Shingleton 2012). To examine if the adult body components of *Actβ* mutants are proportionally reduced, we collected 1-day-old escaper males and females, and measured various traits. We found that the $Act\beta^{80}$ homozygous male weights were reduced on average 28% compared to the control (Figure 2A, female 20% not shown). We next measured the abdomen, thorax, and prothoracic leg lengths, along with head projection and wing surface areas of *Actβ* mutant males and controls. Interestingly, the sizes of some adult structures of *Actβ* mutants were more severely affected than others (Figure 2, B–L). The abdomen length in *Actβ* mutants was reduced by a much greater proportion, −24% (Figure 2, D and F), than any other measured component: head projection area, −8% (Figure 2, B and C); thorax length, −4% (Figure 2, D and E); prothoracic

leg length, −2% (Figure 2, G and J); and wing area −4% (Figure 2, H and K). Using the wing trichome density as a proxy, we found no difference in cell size between *Actβ* mutants and the w^{1118} control (Figure 2, I, K, and L), indicating that the minor reduction in wing size is likely caused by a subtle defect in cell proliferation at some time during development.

Actβ disproportionately affects larval muscle and certain polyploid tissue sizes

To understand the size discrepancies of adult structures in $Act\beta^{80}$ mutants, we examined directly the sizes of various larval tissues including the brain, wing and leg discs, and body-wall muscles, and indirectly the sizes of several polypoid tissues including the fat body, proventriculus, salivary, and PG cells using the size of the nucleus as a proxy for cell size.

The most pronounced defect of $Act\beta^{80}$mutant larvae was exhibited by the body-wall muscles, which in males were reduced by 37% (Figure 3, A–C), and muscle nuclear size by 53% (Figure 3, D–F). The muscle size reduction was not caused by an earlier myoblast fusion defect since mutant muscles contained the same number of nuclei as wild-type (Figure S1). In contrast, neither the brain volume (Figure 3, J and K) nor the 2D-projected surface areas of the wing, leg, and haltere disc (Figure 3, K–P) were significantly affected. Interestingly, we note that the nucleus maximum 2D projection area of several other polyploid tissues, including the fat body and the PGs, were also significantly reduced, but to a lesser degree than the muscle nuclei [22% for the fat body (Figure 3, G–I) and 37% for the PG (Figure S2, G–I)]. Curiously, the nuclear sizes of the cells within the proventriculus and salivary glands are actually slightly and substantially increased, respectively (Figure S2, A–F). We conclude that the small pupal volumes and reduced escaper weights are primarily due to the disproportionate reduction in muscle size, rather than alterations in mitotic tissue growth such as the brain and imaginal discs.

Actβ mutants feed normally but grow slowly

Body size is largely determined by two factors, the duration of growth and the growth rate, or some combination of the two parameters. In addition, a slower growth rate may reflect reduced food intake, diminished absorption of nutrients, or an alteration in metabolic flux. We examined several of these parameters to determine if they were altered in *Actβ* mutants. First, we measured the larval growth rate during the L3 period, when most of the larval growth occurs. At the start of the L3 stage, there was no difference in mass of the mutants *vs.* the controls; however, over the course of 36 hr, a slower rate of mass accumulation became apparent such that, at the time when larvae began to wander, the $Act\beta^{80/80}$ and $Act\beta^{4DD/10E}$ mutants weighed 18 and 17% less than w^{1118} controls, respectively (Figure 4A). This difference in growth rate likely accounts for a large portion of the reduced body size phenotype. To examine whether the diminished growth rate might reflect reduced food intake, we measured feeding rates of foraging early L3 larvae by the mouth-hook contraction assay (Wu *et al.* 2003, 2005). Surprisingly, we found no difference in the head contraction rates of the *Actβ* mutants (Figure 4B), suggesting that the slow growth rate of these mutants is not likely caused by reduced food intake, but instead may reflect an alteration in nutrient absorbance or dysfunctional metabolic flux.

Next, to determine whether the small body size might also involve a reduced growth period, we measured the time to pupariation as well as the critical weight (CW), which is a nutritional checkpoint that ensures larvae have enough nutrient stores to produce viable adults (Nijhout and Callier 2015). In both the control and $Act\beta^{80}$ mutant, starvation after just 2 hr into the L3 stage blocked pupariation (Figure 4C). In the $Act\beta^{80}$ mutant, starvation between 4 and 12 hr after L2/L3 ecdysis resulted in delayed pupariation, and 12 hr after L3, ecdysis starvation resulted in no developmental delay, indicating attainment of CW (Figure 4D). The w^{1118} control achieved CW 8 hr after L2/L3 ecdysis (Figure 4D). At the time when $Act\beta^{80}$ mutants and the w^{1118} control reached CW, we detected no difference in larval weight (0.88 mg for w^{1118} *vs.* 0.84 mg for $Act\beta^{80}$, Figure 4E). Therefore, we conclude that $Act\beta^{80}$ does not affect the CW checkpoint.

Although the CW represents the threshold of mass necessary for pupariation without delay, body size can be altered by either a shorter or longer terminal growth period, which occurs after CW has been reached (Nijhout and Callier 2015). Therefore, we also measured the total time from L2/L3 ecdysis to pupariation. We found that both $Act\beta^{80/80}$ and $Act\beta^{4DD/10E}$ homozygous mutants pupariated slightly earlier than w^{1118} at 25°, but the change was not statistically significant. Moreover, $Act\beta^{4DD}/+$ larvae pupariated significant earlier than w^{1118} control flies (Figure 4F). To test whether the minor change on developmental timing derived from the *Actβ* mutant alleles, we further measured the developmental timing of *Actβ* heterozygous mutants with the *unc13* balancer. The pupariation timing of $Act\beta^{80}$*/unc13* and $Act\beta^{4dd}$*/unc13* larvae did not show any significant change compared with w^{1118} animals (Figure 4F). Unexpectedly, *+/unc13* larvae pupariated slightly, but significantly, earlier than w^{1118} flies, phenocopying $Act\beta^{4DD}/+$ heterozygous mutants (Figure 4F). Therefore, we conclude that while there may be a slight advancement in developmental timing of *Actβ* mutants, differences in genetic background might also account for the small change in the developmental timing of $Act\beta^{80}$ homozygous mutants.

Overexpression of Actβ in its normal pattern produces larger and slower-growing larvae

Since loss of *Actβ* results in small developmentally arrested pupae, we asked whether overexpression of *Actβ* in its endogenous pattern would have the opposite effect on pupal size, viability. For this purpose, we overexpressed *Actβ* using several different *Actβ-Gal4* promoter enhancer lines that all show similar tissue expression patterns, but which vary significantly in the strength of the overexpression depending on insertion site (Figure S3, A and B) (Zhu *et al.* 2008; Song *et al.* 2017a). Relative to either the *UAS-Actβ-3B2* or the *Actβ-Gal4* alone controls, overexpression of most lines (four of six

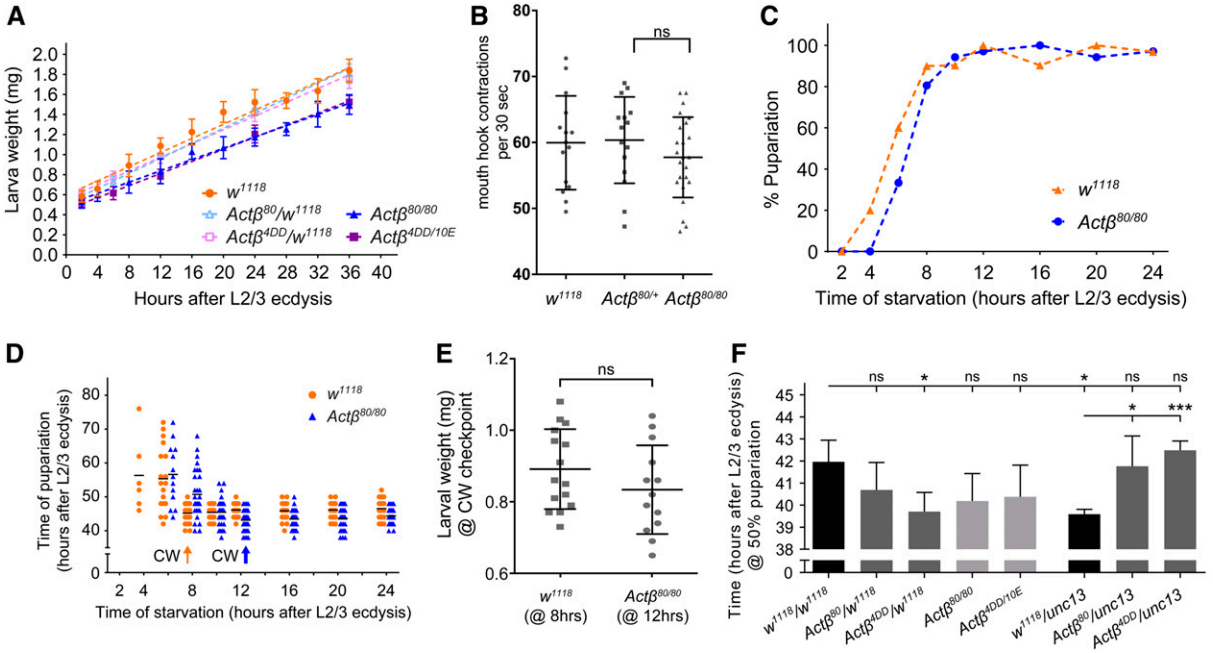

Figure 4 *Actβ* mutant larvae grow slowly but do not exhibit differences in CW or developmental timing. (A) *Actβ* mutants, heterozygotes, and w^{1118} control larvae were synchronized at L2/L3 ecdysis, then larval wet weights were measured at various time intervals. $Actβ^{80/80}$ and $Actβ^{4DD/10E}$ mutants weighed the same as w^{1118} controls immediately after L2/L3 ecdysis (AL2/3 ecdysis), but after 36 hr weighed ∼18% and 17% less than controls, respectively (n = 8–12 per group). $Actβ^{80}$/+ and $Actβ^{4DD}$/+ heterozygotes do not show a difference in growth rate compared with w^{1118} (n = 10–12 per group). (B) A mouth hook contraction assay of early L3 larvae found no difference in feeding rates of $Actβ^{80/80}$ mutants (triangles) *vs.* w^{1118} or $Actβ^{80}$/+ controls (circles and squares) (n = 15–18). (C) *Actβ* mutants are more sensitive to starvation in the early L3 stage than controls. (D) The critical weight checkpoint is determined by identifying the time at which starvation does not delay pupariation. w^{1118} and *Actβ* reach CW 8 and 12 hr, respectively, after L2/L3 ecdysis. (E) Comparing the larval mass at CW checkpoints shows that *Actβ* mutants (at 12 hr AL2/3) weigh the same as controls (at 8 hr AL2/3). (F) Developmental timing analysis of *Actβ* mutants, heterozygotes, and controls. *Actβ* homozygous mutants do not develop significantly faster than the w^{1118} control; however, $Actβ^{4dd}/w^{1118}$ and *unc13GFP*/w^{1118} heterozygotes develop ∼3 hr faster than w^{1118} control. Unless indicated, mean ± SD is shown. * $P < 0.05$ and *** $P < 0.001$. CW, critical weight; ns, not significant.

tested) produced early lethality in which first- and second-instar larvae left the food, and died on the vial wall. One of the weak lines (*Actβ-Gal4-13A3* >) when crossed to *UAS-Actβ-3B2* produced viable flies that exhibited a significant increase in pupal volume (Figure 5A). Strikingly, pupariation is delayed over 20 hr compared to either w^{1118} or *Actβ* mutants; however, there is no change in viability (Figure 5, B and C). The prolonged developmental delay may account for the increased body size of these individuals or the size increase might result from direct growth simulation of muscles. In either case, the cause of the pronounced developmental delay is unclear. We suspect it might be from overexpression in the PTTH neurons (see below), since we have previously shown that activation of Activin signaling in the PG causes significant developmental delay (Gibbens *et al.* 2011). Together, the loss- and gain-of-function data suggest that *Actβ* regulates body size, and perhaps developmental timing, in a dose-dependent manner.

Endogenous Actβ expression identifies several potential sources of Actβ for controlling body size

To investigate how Actβ affects body size, developmental timing, and viability, we first sought to determine if one or more cell types serve as the source(s) of the ligand that controls different aspects of the mutant phenotype. Several features of endogenous *Actβ* transcription have been previously described including expression in motoneurons, mushroom body neurons, peripheral neurons including multi-dendritic and chordotonal neurons, developing photoreceptors in the eye disc, and in midgut enterocytes (Gesualdi and Haerry 2007; Ting *et al.* 2007, 2014; Zhu *et al.* 2008; Kim and O'Connor 2014; Makhijani *et al.* 2017; Song *et al.* 2017a). We examined the *Actβ* expression pattern in the larvae by crossing an *Actβ-Gal4* to *UAS-cd8GFP* or *UAS-GFP*. We also confirmed expression in particular cell types using RNA *in situ* hybridization (Figure S4). As previously described, *Actβ* is almost exclusively expressed in the CNS and PNS (Figure 6E). More detailed examination reveals that in the central brain lobes, *Actβ-Gal4* > *UAS-GFP* is expressed strongly in mushroom body neurons and in a 14-cell cluster in the anterior medial region of each brain lobe (Figure 6, A–A"). A subset of seven cells within this 14 cell-cluster also stain with α-Dilp5 (Figure 6A'), which marks the approximately seven insulin-producing cells (IPCs) (Brogiolo *et al.* 2001). In the ventral nerve cord, *Actβ* >Gal4 is expressed strongly in the motoneurons, marked by α-p-Mad (Figure

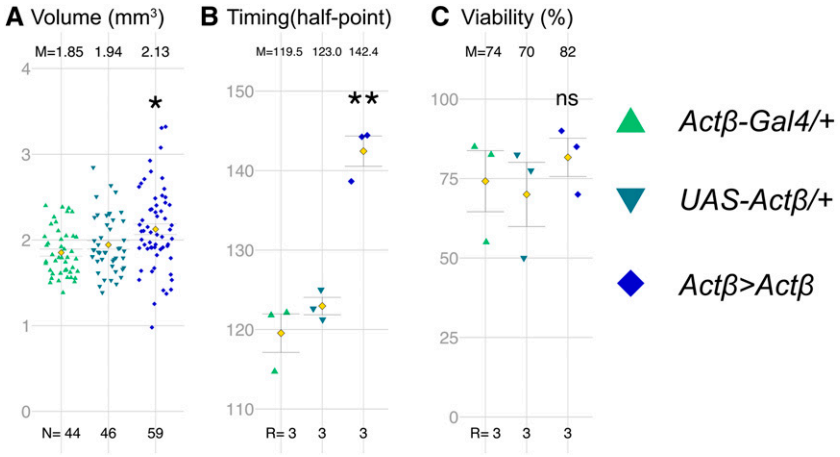

Figure 5 Actβ overexpression increases body size and delays developmental timing. (A) Expression of *UAS-Actβ* using *Actβ-Gal4* significantly increases pupal volume. (B) *Actβ Gal4-13A3 >Actβ* animals pupariate about ~20 hr later than controls. (C) Adult viability is not significantly impacted in *Actβ Gal4-13A3 > Actβ* animals. M, mean; N, number of individuals; R, number of groups containing 30–40 larvae; UAS, upstream activating sequence.

6, G–G") (Marqués *et al.* 2002). We also see strong staining in all α-DIMM-marked neuroendocrine cells (Figure 6, H–H") (Park *et al.* 2008).

Because of the possible developmental timing defects, we were particularly interested in whether *Actβ* is expressed in the neurons that innervate the ring gland (RG), the major endocrine organ of larvae, or in any of the RG cells themselves. We found strong expression in the corpus cardiacum (CC) cells that produce the hormone Akh, which is involved in regulating sugar metabolism (Figure 6, C–C" and Figure S4D) (Lee and Park 2004). While we observed no expression in the cells of the PG, which produces the steroid hormone ecdysone (Yamanaka *et al.* 2013a), or in the corpus allatum (CA), which produces JH (Riddiford *et al.* 2010), we did see signal in axons tracts that innervate each of these tissues (Figure 6, F–F'). The PG neurons produce PTTH and innervate the PG portion of the RG to regulate ecdysone production (Siegmund and Korge 2001; McBrayer *et al.* 2007). Costaining of *Actβ>nucGFP* brains with α-PTTH reveals strong expression in the PG neurons (Figure 6, B–B"). While we have no specific antibody that marks the CA neurons, the GFP-positive innervations that we observe on the CA are highly suggestive that the CA neurons express Actβ (Figure 6, F–F'). Actβ is also found in various other unidentified neurons within the central brain and ventral nerve cord. Outside the CNS and PNS, we observe Actβ expression only in a limited number of enterocytes in the midgut (Figure 6, D–D" and Figure S4H), as previously reported (Song *et al.* 2017a), the adult ovariole follicle and border cells (Figure 6, I and J and Figure S4G), some tracheal-associated cells (Figure 6K and Figure S4F), and the differentiating photoreceptors of the eye (Figure 6L and Figure S4C). Our observation that the rare escaper females are fertile suggests that Activin signaling in the follicle cells is either not required for full fertility or that its expression might be redundant with another Activin-like ligand, such as Dawdle or Myoglianin.

Motoneuron-derived Actβ regulates body size and viability

To determine which *Actβ*-expressing cell types influence size and viability, we attempted rescue experiments using different tissue-specific Gal4 drivers to overexpress the *Actβ* transgene in the $Actβ^{80}$ mutant background. $Actβ^{80}$ mutants with one copy of either the *UAS-Actβ* or the various *Gal4* transgenes served as negative controls. Since overexpression of *Actβ-GAL4* driving *UAS-Actβ* is sufficient to increase body size (Figure 5A), here we asked whether it is able to rescue the small body size (pupal volume) and pupal lethality of *Actβ* mutants. Indeed, *Actβ-Gal4-2A2> UAS-Actβ3B2* in the mutant background is not only sufficient to rescue body size, but actually produces larger animals (12% bigger than wild-type, Figure 7A), similar to what we see upon overexpression in a wild-type background (Figure 5A). Overexpression of Actβ in its normal pattern also resulted in strong but not complete rescue of lethality (Figure 7B, 42.7% viability *vs.* 1–4% viability of mutant controls; the test cross viability rate for w^{1118} is 73.8%, Figure 7B). The reason for incomplete rescue of viability, despite muscles being larger, is not readily apparent. However, it may indicate that various processes within a tissue respond differently to a particular level of Actβ. For example, Actβ not only regulates muscle size (this report), but it also alters muscle physiology (Kim and O'Connor 2014). Thus, overexpression may perturb these two functions in different ways potentially leading to a partially defective motor program.

To narrow down the relevant source of ligand that regulates each phenotype, we used increasingly restrictive (tissue-specific) Gal4 lines to overexpress *Actβ*, and then measured body size and viability. Overexpression of *Actβ* using the pan-neuronal driver, *nrv2-Gal4*, rescues both body size and adult viability (Figure 7, C and D). Surprisingly, overexpression of *Actβ* from the motoneurons *OK371 > GAL4* alone rescues both body size and viability (Figure 7, E and F). Interestingly, *Actβ* overexpression in $DIMM^+$ neuroendocrine cells (*C929 > Gal4*) also rescues both body size and viability (Figure 7, G and H). Just like overexpression of *Actβ* from its endogenous sources, we also found that overexpression of *Actβ* in either motoneurons or neuroendocrine cells in wild-type animals also produces large adults (Figure S5). Lastly, overexpression of *Actβ* in only the IPCs (*dilp2 > Gal4*), which makes up a much smaller subset of all neuroendocrine cells, does not rescue either phenotype (Figure 7, I and J).

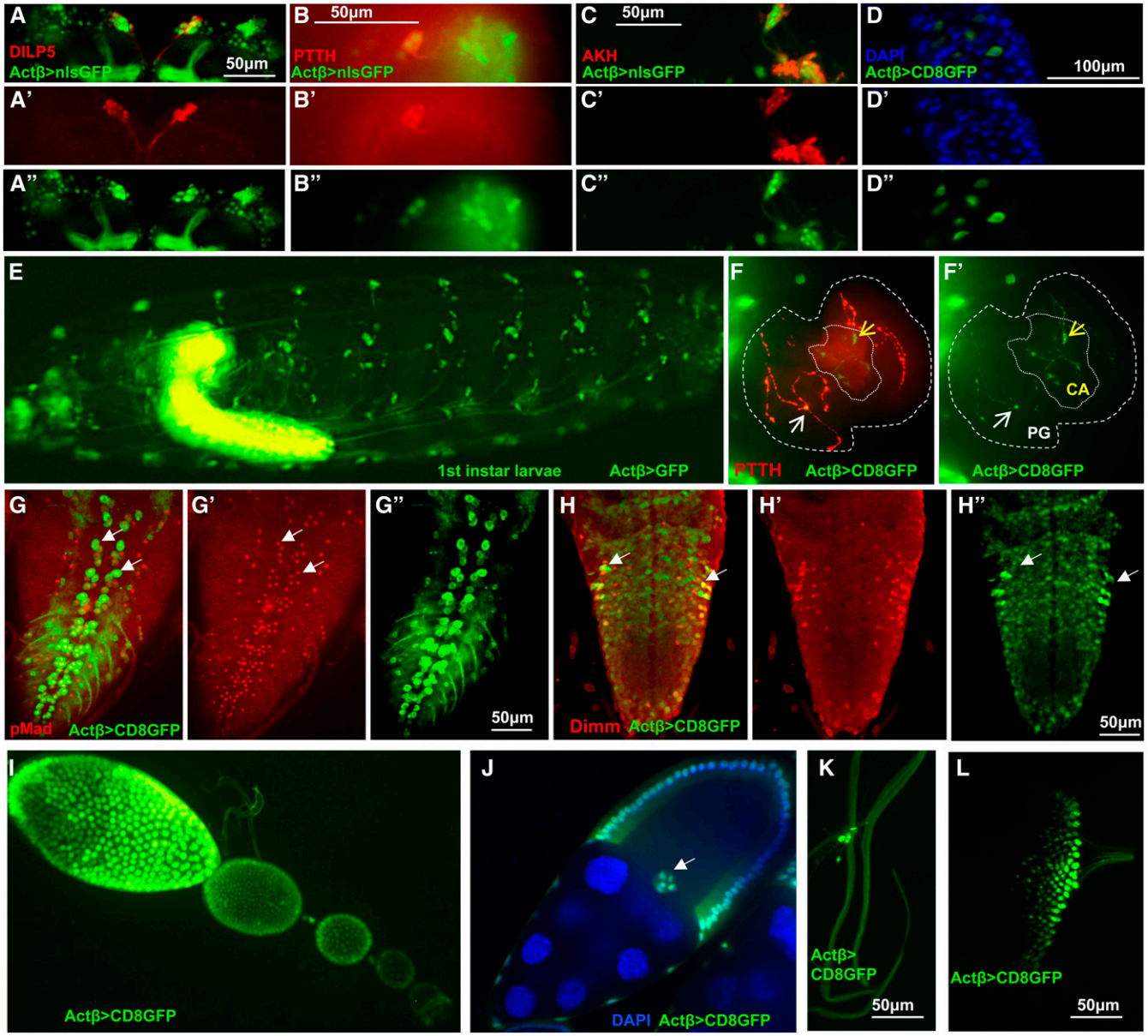

Figure 6 Analysis of *Actβ-GAL4* driver expression pattern (green) in L3 larvae and female ovaries. (A–A'') *Actβ-GAL4-2A2* is expressed in the insulin-producing cells in the central brain, marked with α-Dilp5 (red). (B–B'') *Actβ* reporter is expressed in the cell bodies of PTTH neurons (α-PTTH, red) in the central brain. (C–C'') *Actβ* reporter is expressed in Akh-producing (α-AKH, red) neurons. (D–D'') *Actβ-Gal4*-driven GFP is expressed in midgut enteroendocrine cells (blue, DAPI). (E) An intact L1 larva, *Actβ-Gal4*-driven GFP is expressed in both the CNS and PNS. (F and F') *Actβ-Gal4-2A2*-driven GFP is found in PTTH synaptic boutons (red) on the PG (thicker dotted line, white arrows) as well as unique boutons in the CA (finer dotted line, yellow arrows). (G–G'') *Actβ* reporter drives expression in the motor neurons (marked with α-pMad red) in the ventral nerve cord (white arrows highlight two individual motor neurons). (H–H'') *Actβ* reporter is expressed in neuroendocrine cells (α-DIMM, red) in the ventral nerve cord. (I and J) *Actβ-Gal42A2*-driven GFP is found in follicle cells and the border cells [white arrow in (J)] during egg development. (K) *Actβ-Gal4-2A2*-driven GFP is found in certain tracheal-associated cells (likely neuroendocrine Inka cells) and (L) in differentiating photoreceptor cells in the eye disc. ** $P < 0.01$, *** $P < 0.001$, and **** $P < 0.0001$. CA, corpus allatum; ns, not significant; PG, prothoracic gland; PTTH, prothoracicotropic hormone.

The finding that expression in only the motoneurons rescues body size suggests that Actβ may be supplied directly to the muscles via the neuromuscular junctions. However, we also find that overexpression in neuroendocrine cells is sufficient to rescue body size, which suggests that Actβ may be able to function as a systemic endocrine signal and need not be directly delivered to the muscle via the neuromuscular junction synapse. Therefore, we asked if expression of *Actβ* from nonneuronal, but highly secretory, tissues was able to rescue various aspects of the null phenotype. Interestingly, expression of *Actβ* using the *ppl-Gal4* (fat body and muscle) driver increases pupal volume beyond wild-type levels and partially rescues adult viability (Figure 7, K and L). Overexpression in only the body-wall muscles (*MHC-Gal4*) also

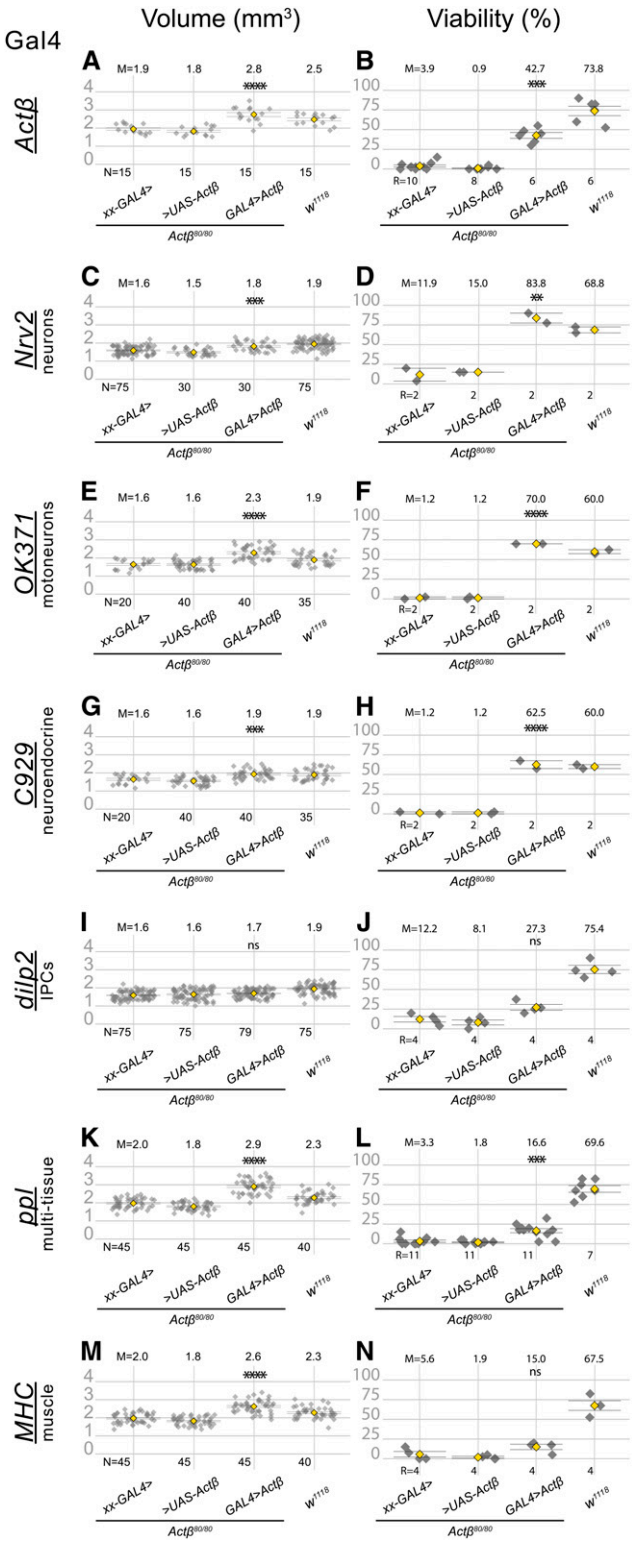

Figure 7 Expression of Actβ from specific cell types differentially rescues the pupa size (A, C, E, G, I, K and M) and viability (B, D, F, H, J, L and N) phenotypes in Actβ mutants. The first two groups in each panel are controls in which *Actβ* mutants contain one copy of either the GAL4 driver (indicated on the left side of each panel row) or the UAS Actβ transgene. The third group in each panel is the test cross, and the last group in each panel is the w^{1118} control. All GAL4 drivers (except *dilp2-GAL4)* used to overexpress *Actβ* rescue body size phenotype (A, C, E, G, K, and M). Overexpressing *Actβ* in neuronal tissues (D, F, and H) completely rescues the adult viability phenotype and partially rescues it when overexpressed in body-wall muscles using MHC-GAL4 (L). ANOVA was used to determine statistical significances between genotypes with one copy of either the Gal4 or UAS transgene in an $Actβ^{80}$ homozygous background, compared to animals with both Gal4 and UAS transgenes in an $Actβ^{80}$ homozygous background. w^{1118} is the wild-type control and was reared side-by-side in each case. M, mean; N, number animals; R, repetition number (10–30 animals per repetition); UAS, upstream activating sequence.

increases body size beyond wild-type levels, but does not rescue adult viability (Figure 7, M and N). However, we note that overexpression of *Actβ* using either *MHC-Gal4* or *ppl-Gal4* in a wild-type background results in most animals dying as large oversized and curved pupae (Figure S6). These phenotypes are likely due to hyperactivation of TGF-β signaling in the muscles because we observe a similar phenotype when a constitutively activated version of Babo is overexpressed in the muscles (Figure S6). Taken together, these results suggest that, although Actβ signaling in muscles is required for proper body size, too much signaling in muscles can be deleterious. We were not able to specifically test the ability of enteroendocrine-derived Actβ to rescue mutant phenotypes, because overexpression of *Actβ* using the midgut enteroendocrine cell driver (*EE-Gal4*) (Song *et al.* 2017a) is lethal in both wild-type and *Actβ* mutant backgrounds, likely due to overexpression in many cells besides enteroendocrine cells, including the fat body, CNS, and PNS (data not shown). In summary, we conclude that since overexpression of Actβ from motoneurons or neuroendocrine cells rescues both body size and viability, and can increase body size when overexpressed from these sources in wild-type animals, they are likely the most important endogenous sources of ligand for viability and body size control.

Motoneuron-derived Actβ signals through the canonical Babo/dSmad2 pathway to control muscle and body size

The rescue experiments described above suggest that either motoneurons or DIMM$^+$ neuroendocrine cells, or both, can produce enough Actβ to regulate body size. Since data from overexpression alone do not reflect the *in vivo* importance of various endogenous ligand sources, we sought a complementary set of loss-of-function data using tissue-specific RNAi knockdown. First, we tested all publicly available (the Transgenic RNAi Project (TRiP), Vienna *Drosophila* Resource Center, and National Institute of Genetics (NIG)] *Actβ* RNAi lines to phenocopy the *Actβ* mutant. Using the ubiquitous driver da-*GAL4* to overexpress *dicer2* along with the various *Actβ* RNAi lines, we found that only the TRiP stock (BDSC#29597) could phenocopy the small, dead pharates similar to *Actβ* null alleles (data not shown). Most other lines produced viable flies of normal size, suggesting that they are not very effective in knocking down endogenous *Actβ*. Both NIG lines (1162R-1 and 1162R-2) produced a more severe

phenotype (early larval lethality) compared to the null suggesting they may have off-target effects.

Using the TRiP 29597 RNAi line, we tested whether knockdown of *Actβ* in either all neurons, motoneurons, or neuroendocrine cells alone phenocopied any aspect of null alleles. We found that knockdown in DIMM$^+$ neuroendocrine cells (*C929-Gal4*) produced viable normal-sized flies (Figure S7). In contrast, knockdown in all neurons (Elav > Gal4 Figure 8A) or motoneurons (*OK371-Gal4*, Figure 8, A and B) completely phenocopied *Actβ* nulls, giving rise to small, dead pharates with rare escapers that held out their wings and had a slow gait (Movies S3 and S4). The *OK371* driver was not expressed in the DIMM$^+$ neuroendocrine cells (Figure S8), leading us to conclude that the motoneurons are the major source of endogenous *Actβ* that regulates body size and viability.

We next determined if motoneuron-derived *Actβ* signals to the muscle via the canonical Smad2 pathway. Canonical TGF-β signaling is mediated by the Activin receptor Babo and the signal transducer dSmad2. In muscles, overexpressed Babo is localized to the postsynaptic neuromuscular junction, perhaps sensitizing the muscles to receive motoneuron-derived Actβ (Kim and O'Connor 2014). Indeed, RNAi knockdown of *babo* or *dSmad2* in the body-wall muscle resulted in smaller pupal volume (Figure 8, C and D). Furthermore, on Western Blots, we detected lower levels of phosphorylated dSmad2 in *Actβ* mutant carcass extracts (containing somatic muscle, cuticle, and associated cells) compared to the w^{1118} control (Figure 8E) and overexpression of *Actβ* in motoneurons both increased pupal/adult size (Figure S5) and p-Smad2 levels in the carcass (Figure 8, D and E). Overexpression of activated dSmad2 in the muscle enhances muscle size producing flies with extended abdomens (Fig. 8F-H) as does overexpression of activated Babo in muscles (Figure S9, A-C). Interestingly, the *MHC > dSmad2(SDVD)* animals with larger body size had slightly smaller wings, not larger wings as expected, if organs were actively scaled to maintain size proportions between muscles and appendages (Figure S9D).

Discussion

Identifying and characterizing how interorgan signals regulate physiologic and metabolic homeostasis, during development and adulthood, is of central importance. Various types of interorgan signals are also likely to be necessary for coordinating growth between organs during development to achieve proper body proportions (Droujinine and Perrimon 2016). In this report, we demonstrate that Actβ is a key brain-derived factor that regulates somatic muscle size in *Drosophila* by signaling through the canonical Smad-dependent pathway. Furthermore, we find that disruption of Actβ signaling alters larval and adult organ allometry, suggesting that Actβ might be a component of an interorgan signaling pathway that helps coordinate muscle growth with appendage growth.

Localized vs. systemic effects of Actβ

The question of whether Actβ acts locally or systemically via the hemolymph to target tissues is an important issue raised by our study and previous work (Song *et al.* 2017a,b). On the one hand, we find that *Actβ* is strongly expressed in most if not all neuroendocrine cells. We also find that overexpression of *Actβ* from these cells results in the rescue of mutant phenotypes and overgrowth of wild-type animals, indicating that direct tissue contact is not necessary for Actβ signaling to control muscle size. However, we also find that depleting *Actβ* expression in just the motoneurons phenocopies *Actβ* mutants while depletion in neuroendocrine cells does not do so, at least with the *929 > Gal4* driver. Therefore, we conclude that, while high systemic concentrations of Actβ produced by overexpression are capable of regulating muscle growth, the endogenous systemic level supplied by the combination of the neuroendocrine and the enteroendocrine cells is not sufficient to do so.

Whether local or systemic Actβ signaling is important in other contexts is less clear. Interestingly, Actβ has also been implicated in regulating hemocyte proliferation and adhesion within hematopoietic pockets localized on the larval body surrounding a number of peripheral neurons that express *Actβ*, including da and chordotonal peripheral neurons (Makhijani *et al.* 2017). In contrast, enteroendocrine-derived Actβ is able to affect Akh receptor levels in the fat body to regulate glycemic index on a high-sugar diet (Song *et al.* 2017a). In addition, it has been reported that upon mitochondrial perturbation, muscle-derived Actβ signals to the fat body to regulate triglyceride levels (Song *et al.* 2017b). In either case, these observations raise the question: what dictates the requirement of a local *vs.* a systemic signal for Actβ function? In the muscle motoneuron synapses and hematopoietic pocket paradigms, there may be physical barriers that help concentrate ligand from a local source to levels sufficient to produce a response. In the case of muscles, motoneuron synapses are embedded within the muscle fiber (Prokop 2006; Prokop and Meinertzhagen 2006) and therefore delivery of Actβ directly to the neuromuscular junction (NMJ) via the synapse likely provides a highly effective signal, especially since its receptor Babo is also highly concentrated at the postsynaptic NMJ (Kim and O'Connor 2014). This possibility might also account for the discrepancy between our findings (Figure S4) that muscles do not express Actβ under normal conditions, while mitochondrial perturbations in muscle appear to release Actβ for signaling to the fat body (Song *et al.* 2017b), perhaps disturbing mitochondrial function in muscle disrupts synaptic structure such that Actβ is liberated from defective NMJ synapses. Likewise, the hematopoietic pockets might provide a similar restricted niche-like signaling environment that is able to modulate hemocyte proliferation and adhesion. These types of physical constraints may limit the ability of endogenous circulating Actβ to produce sufficient levels of signaling at these locations, except under overexpressed conditions.

Another factor influencing the cellular response to Actβ levels is the composition of the surface receptors. The *babo* locus produces three receptor isoforms that only differ in the extracellular ligand-binding domain, and each likely has a

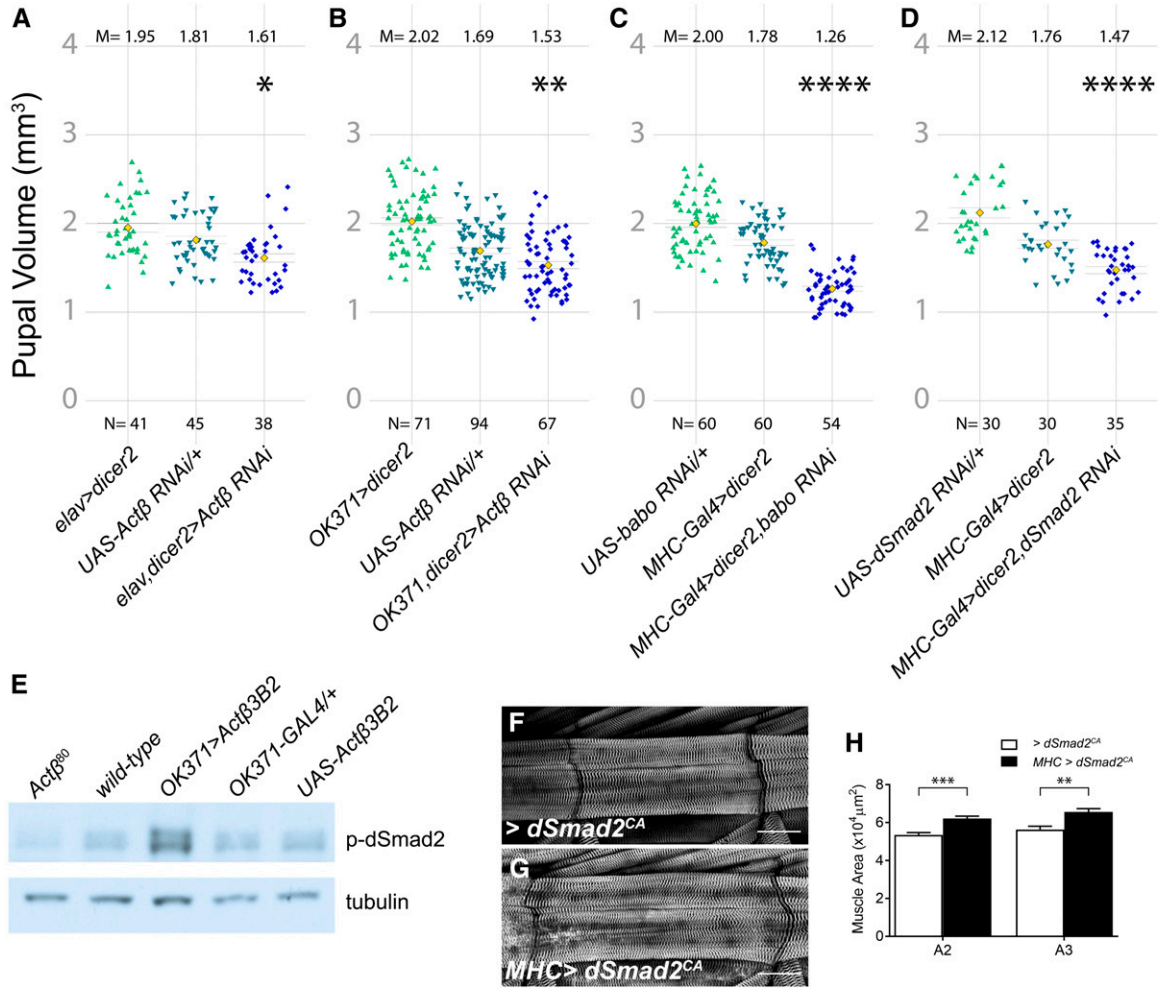

Figure 8 Motor neuron-derived Actβ signaling through Babo and dSmad2 controls body size. (A). Knockdown of *Actβ* using a pan-neuronal driver (*elav-Gal4*) with *UAS-dicer2* reduces pupal volume. (B) Motor neuron knockdown of *Actβ* using *OK371-Gal4* also reduces pupal volume. In both (A and B), the control containing the UAS Actβ RNAi line on its own is also significantly smaller than the driver-alone control line. We speculate that this is caused by leaky non-Gal4-driven expression of the *UAS-Actβ* RNAi line, a phenomenon that we have previously encountered when using certain other UAS lines. (C) Knocking down the *Actβ* receptor *baboon* or the signal transducer *dSmad2* (D) in muscles using *MHC-GAL4* with UAS-*dicer2* reduces pupal volume. (E) *Actβ* mutants have lower levels of p-dSmad2 [(E) lanes 1 *vs.* 2] in carcass tissue lysates (cuticle, skeletal muscle), while overexpressing Actβ in motor neurons leads to increased levels of dSmad2 compared to controls [(E) lanes 3–5]. Anti-tubulin staining serves as a loading control. (F–H) Overexpressing constitutively activated dSmad2 (dSmad2^{CA}) in the muscles using *MHC-GAL4* increases muscle size by ~20%. M, mean; N, number; RNAi, RNA interference; UAS, upstream activating sequence.

different affinity for the three Activin-like ligands (Jensen *et al.* 2009; Upadhyay *et al.* 2017). Therefore, the complement of receptor isoforms on a cell's surface is apt to determine the sensitivity of the cell or tissue to Actβ signals.

Mechanisms of Actβ control of tissue size

The molecular mechanism(s) by which Actβ affects tissue growth are unclear. The most well-characterized factors that regulate insect body size are all systemic signals such as JH, ecdysone, and the IIS/TOR pathways (Rewitz *et al.* 2013; Mirth and Shingleton 2014; Boulan *et al.* 2015; Koyama and Mirth 2018). For example, *Ptth* mutants delay ecdysone accumulation allowing larvae to grow for an additional 24 hr, ultimately leading to larger flies (Shimell *et al.* 2018). In this report, we demonstrate that Actβ, although it is expressed in the PTTH-producing neurons, does not appear to affect ecdysone signaling since *Actβ* loss affects neither CW nor developmental timing.

Interestingly, we also see Actβ-positive innervation of the CA organ, which produces JH, and lowering JH levels in *Drosophila* leads to the production of smaller flies by slowing the overall growth rate (Riddiford *et al.* 2010; Mirth *et al.* 2014) Since we also observe a slower growth rate in *Actβ* mutants, it is possible that Actβ might work to slow growth via reduction of JH signaling. However, given the strong expression of Actβ in all DIMM^{+} neuroendocrine cells, which secrete numerous behavior and metabolism modifying peptides including insulin, many other mechanisms for slowing growth must be considered. While food intake does not seem to be altered in Actβ mutants, it is possible that nutrient

absorption or metabolic flux is disrupted. The latter possibility is particularly attractive since we see strong expression of *Actβ* in the CC organ, which produces the *Drosophila* glucagon-like hormone (Akh), and in the IPCs in the brain. As previously noted, Actβ has been implicated in regulating Akh receptor levels in the fat body (Song *et al.* 2017a), and it may also influence Akh synthesis or release. Furthermore, Dawdle, another *Drosophila* Activin-like ligand that also signals through dSmad2, has been previously shown to regulate metabolism and carbohydrate utilization (Chng *et al.* 2014; Ghosh and O'Connor 2014). Therefore, Actβ signaling through dSmad2 may also regulate global carbohydrate synthesis or aspects of metabolism to adjust the larval growth rate.

Regardless of how overall growth defects occur, it is important to remember that not all larval tissues respond equally to Actβ. The brain and imaginal discs, for example, are of normal size, while the fat body and muscle are significantly smaller. In addition, the size and viability defects can be largely rescued by the expression of Actβ solely in motoneurons. Therefore, it seems unlikely that a primary defect in systemic levels of insulin or Akh would account for the tissue-specific responses. Rather, it is likely that alterations in muscle metabolism and perhaps factors secreted by muscles could account for the small muscle/body size.

Larval vs. adult requirements for Actβ

The requirement of Actβ for adult eclosion raises several issues. The first is whether the low eclosion rate is primarily a muscle defect or a neuronal problem, since both must be coordinated to produce the complex set of motor behaviors required for eclosion. Interestingly, ablation of $DIMM^{+}$, eclosion hormone-producing neuroendocrine cells (Park *et al.* 2008) results in a defective eclosion motor program, which involves a series of coordinated head, thorax, and abdominal muscle contractions that eject the animal through the operculum and out of the pupal case (McNabb *et al.* 1997). It may be that the small adult muscles lack the power to properly execute the eclosion motor program. In addition, the small muscle phenotype may also partially explain why the *Actβ* mutant adult escapers walk slowly and cannot move their wings. However, this must be reconciled with the observation that *Actβ* mutant larvae exhibit no obvious defect in locomotion, even though they have a similar proportional reduction in overall body and muscle size.

Improper synaptic development or NMJ function could also potentially account for adult locomotion defects. However, we have previously shown that, at least in larvae, the NMJ size and bouton number are not affected in *babo* and *dSmad2* mutant larvae when normalized to the smaller muscle size (Kim and O'Connor 2014). Nevertheless, we did uncover a number of electrophysiological alterations, including a decrease in the number and frequency of miniature excitatory potentials, and a depolarized muscle membrane resting potential, both of which were primarily attributed to defective Actβ signaling in muscles (Kim and O'Connor 2014). Despite these defects, the large action potentials in *babo* and *dSmad2* mutants are relatively normal and, as described, there are no obvious larval locomotion defects (Kim and O'Connor 2014). Since adult muscles are formed *de novo* during metamorphosis, it is possible that during this time more extreme defects in muscle or neuron physiology develop in *Actβ* mutants, perhaps leading to a more strongly depolarized muscle, for example, that would interfere with proper muscle function.

The motoneuron source of Actβ also raises questions concerning whether Actβ production/release is muscle/neuron activity-dependent. We find that overexpression of Actβ in motoneurons can produce bigger muscles, but whether increased muscle activity also accompanies higher Actβ expression/secretion triggering increased muscle growth is an interesting issue to address. However, we note that adult muscles, which develop during the immobile pupal stage, are also likely smaller than wild-type in *Actβ* mutants, suggesting that significant muscle activity is not likely required for Actβ release.

Body-appendage scaling

One of the more novel features of the *Actβ* null phenotype is the disproportionate effect it has on muscle size compared to other tissues. One might expect that evolutionary pressures fine-tune mechanisms to coordinate muscle size with the size of the appendage that it moves. This is perhaps especially true in winged insects where flight muscle and wing size should be coordinated to produce efficient flight. Such coordination between wing and body size in response to environmental perturbations has been best studied in *Manduca sexta* (Nijhout and Grunert 2010; Nijhout and Callier 2015). In this insect, nutritional restriction can result in a $\leq$ 50% reduction in body size, with the wing scaling proportionally and containing one-half as many cells (Nijhout and Grunert 2010). This scaling mechanism utilizes a shift in the amplitude and kinetics of steroid hormone production during the last-instar stage. Since this mechanism involves systemic factors that adjust the growth rate of the whole body, presumably affecting muscles and discs simultaneously, it does not really address whether specifically perturbing muscle growth can directly or indirectly affect growth of the wing or other appendages.

In *Drosophila*, alteration in the growth properties of one imaginal disc perturbs growth of other wild-type discs in a coordinated manner so that adults emerge with properly proportioned structures (Simpson and Schneiderman 1975; Simpson *et al.* 1980; Stieper *et al.* 2008). Once again, the interorgan signaling mechanism involves alteration in the levels of systemic hormones (Parker and Shingleton 2011; Mirth and Shingleton 2012; Gokhale *et al.* 2016). In these reports, is not clear whether muscle size was also altered to produce isometric scaling between it and the imaginal discs. However, it is interesting to note that growing *Drosophila* at low temperatures produces hyperallometric scaling where the wing size is disproportionally larger relative to body size (Shingleton *et al.* 2009). Since we observe similar phenotypes

in *Actβ* mutants grown at normal temperatures, it is intriguing to speculate that Actβ signaling might mediate hyperallometric scaling between the wing and body in response to temperature.

The only other report that we are aware of where *Drosophila* larval muscle size was specifically manipulated, and the effect on growth of other tissues examined, involved genetic alteration of insulin signaling (Demontis and Perrimon 2009). Similar to our analysis of *Actβ*, the level of insulin signaling in muscle is directly correlated with muscle, appendage, and overall animal size. Nevertheless, our findings for Actβ show several notable differences. First, insulin gain-of-function signaling in muscle leads to larger bodies and larger wings (Demontis and Perrimon 2009), while we find that increased Actβ signaling in muscles results in larger bodies, but slightly smaller wings. In the insulin loss-of-function case, both muscles and wings were smaller, the latter due to a reduction in cell size not cell number. However, in the case of *Actβ* mutants, we see only a 4% decrease in wing size with no change in cell size. In both cases, the effect on muscle size appears to be much more dramatic than the effect on appendage size. Therefore, if a scaling mechanism exists, then either insulin or Actβ loss disrupts it, or it is not isometric as is found for the nutrient-dependent body–wing scaling response in *M. sexta*. The general similarity in phenotypes produced by insulin or Actβ signaling suggests that Actβ may exert its effect on muscle and body size, in part, through the insulin signaling pathway, a possibility that we are currently exploring.

TGF-β control of body size in other animals

TGF-β regulation of body or muscle size has been reported in both *C. elegans* and mammals. In *C. elegans*, BMP-type factors are also secreted from a specific set of neurons and appear to act systemically to regulate the size of the hypodermis through a canonical Smad-dependent pathway (Tuck 2014). In fact, the term Smad is a compound word derived from the *C. elegans* gene *sma*, meaning small, and the *Drosophila* gene *mad* (mothers against dpp), which were the founding members of the Smad family of TGF-β signal transducers (Derynck *et al.* 1996). Recently, many transcriptional targets for the Sma factors in *C. elegans* have been identified, among which are several collagens that are major structural components of the hypodermal body wall (Madaan *et al.* 2018). Hence, we speculate that one set of targets for both Actβ and insulin signaling in the *Drosophila* muscle could be structural proteins that build muscle. It is also possible that target gene expression is indirectly regulated by DNA copy number. In *Drosophila*, larval and adult muscle are polyploid tissues where DNA content is controlled by endocycling. Both Actβ (this report) and insulin signaling (Demontis and Perrimon 2009) appear to regulate nuclear size in many polypoid tissues, possibly indicating that control of the endocycle maybe the primary mechanism regulating tissue size. However, at least in Actβ mutants, not all polyploid tissues show regulation in the same direction, *i.e.*, the muscle, fat body, and the PG all show smaller nuclei while the salivary gland has larger nuclei. Whether systemic Actβ signaling is directly regulating the size of polyploid tissues or acts indirectly through a muscle-derived myokine needs to be determined.

In mammals, the best-characterized example of a TGF-β-type factor that regulates body and muscle size is provided by Myostatin. Loss of Myostatin was discovered to cause the muscle-overgrowth phenotype of Belgian blue cattle and subsequent work in many other species, including humans, has confirmed that Myostatin is a negative regulator of muscle mass (McPherron and Lee 1997; McPherron *et al.* 1997). Muscles *myostatin* mutants have both an increase in myofiber number (Trendelenburg *et al.* 2009; Matsakas *et al.* 2010) as well as of myofiber size (McPherron and Lee 1997; Elashry *et al.* 2009). The molecular basis for the phenotype appears to be an alteration in protein homeostasis, where proteasomal and autophagic degradative capacity is reduced relative to protein synthesis (Lee *et al.* 2011; Lokireddy *et al.* 2012). Myostatin signals through Smads2/3 and is therefore considered to be within the TGF-β/Activin subgroup in the TGF-β superfamily. Additional studies of Activin ligands themselves suggest that that they also act as negative regulators of muscle mass similar to Myostatin (Zhou *et al.* 2010). Furthermore, studies on the role of BMP signals in muscle-size control suggest that they function as dominant positive regulators of muscle mass by promoting protein synthesis instead of breakdown (Sartori *et al.* 2013; Winbanks *et al.* 2013).

Our present work shows that in *Drosophila*, Actβ is a positive regulator of muscle mass, by affecting myofiber size not number. It is worth noting that *Drosophila* has a close Myostatin homolog that is called *myoglianin* (*myo*), and recent studies suggest that loss of *myo* in muscle produces larger fibers similar to the vertebrate homolog (Augustin *et al.* 2017). How Actβ and Myo interact will be interesting to examine, as will the role for BMPs in *Drosophila* muscle-size determination. Lastly, the question of whether Myostatin loss in vertebrates affects scaling of other tissues is largely unexplored, although it does appear that bone density is increased in *myostatin* mutant animals (Elkasrawy and Hamrick 2010). Additional studies of how local *vs.* systemic roles of TGF-β ligands might affect growth and scaling between tissues and organs in vertebrates should be enlightening.

Acknowledgments

We thank Aidan Peterson, MaryJane O'Connor, and Heidi Bretscher for comments on the manuscript; David Zhitomirsky for making guide RNA constructs to generate CRISPR/Cas9 alleles; P. Leopold for the anti-PTTH antibody; P. Taggert for the anti-DIMM antibody; M. Titus for providing the microscope for live imaging of feeding larvae; and the Bloomington *Drosophila* Stock Center for providing numerous fly lines. This work was supported by a National Institutes of Health grant (1R35 GM-118029 to M.B.O.) and an American Heart Association Predoctoral Fellowship grant

15PRE25700041 to L.M.-T. The authors declare no competing or financial interests.

Author contributions: conceptualization: M.B.O. and L.M.-T.; experimentation and data analysis: L.M.-T., A.U., X.P., M.-J.K., and M.B.O.; writing: M.B.O., A.U., and L.M.-T.; and funding acquisition: L.M.-T. and M.B.O.

Literature Cited

Augustin, H., K. McGourty, J. R. Steinert, H. M. Cocheme, J. Adcott *et al*., 2017 Myostatin-like proteins regulate synaptic function and neuronal morphology. Development 144: 2445–2455. https://doi.org/10.1242/dev.152975

Böhni, R., J. Riesgo-Escovar, S. Oldham, W. Brogiolo, H. Stocker *et al*., 1999 Autonomous control of cell and organ size by CHICO, a *Drosophila* homolog of vertebrate IRS1–4. Cell 97: 865–875. https://doi.org/10.1016/S0092-8674(00)80799-0

Boulan, L., M. Milán, and P. Léopold, 2015 The systemic control of growth. Cold Spring Harb. Perspect. Biol. 7: a019117. https://doi.org/10.1101/cshperspect.a019117

Brogiolo, W., H. Stocker, T. Ikeya, F. Rintelen, R. Fernandez *et al*., 2001 An evolutionarily conserved function of the *Drosophila* insulin receptor and insulin-like peptides in growth control. Curr. Biol. 11: 213–221. https://doi.org/10.1016/S0960-9822(01)00068-9

Brummel, T., S. Abdollah, T. E. Haerry, M. J. Shimell, J. Merriam, 1999 The *Drosophila* activin receptor baboon signals through dSmad2 and controls cell proliferation but not patterning during larval development. Genes Dev. 13: 98–111. https://www.ncbi.nlm.nih.gov/pmc/articles/PMC316373/

Chen, C., J. Jack, and R. S. Garofalo, 1996 The *Drosophila* insulin receptor is required for normal growth. Endocrinology 137: 846–856. https://doi.org/10.1210/endo.137.3.8603594

Chng, W. A., M. S. B. Sleiman, F. Schüpfer, and B. Lemaitre, 2014 Transforming growth factor beta/activin signaling functions as a sugar-sensing feedback loop to regulate digestive enzyme expression. Cell Rep. 9: 336–348. https://doi.org/10.1016/j.celrep.2014.08.064

Church, R. B., and F. W. Robertson, 1966 A biochemical study of growth of Drosophila melanogaster. J. Exp. Zool. 162: 337–351. https://doi.org/10.1002/jez.1401620309

De Loof, A., T. Vandersmissen, E. Marchal, and L. Schoofs, 2015 Initiation of metamorphosis and control of ecdysteroid biosynthesis in insects: the interplay of absence of Juvenile hormone, PTTH, and Ca(2+)-homeostasis. Peptides 68: 120–129. https://doi.org/10.1016/j.peptides.2014.07.025

Demontis, F., and N. Perrimon, 2009 Integration of Insulin receptor/Foxo signaling and dMyc activity during muscle growth regulates body size in *Drosophila*. Development 136: 983–993. https://doi.org/10.1242/dev.027466

Derynck, R., W. M. Gelbart, R. M. Harland, C. H. Heldin, S. E. Kern *et al*., 1996 Nomenclature: vertebrate mediators of TGFbeta family signals. Cell 87: 173. https://doi.org/10.1016/S0092-8674(00)81335-5

Droujinine, I. A., and N. Perrimon, 2016 Interorgan communication pathways in physiology: focus on *Drosophila*. Annu. Rev. Genet. 50: 539–570. https://doi.org/10.1146/annurev-genet-121415-122024

Elashry, M. I., A. Otto, A. Matsakas, S. E. El-Morsy, and K. Patel, 2009 Morphology and myofiber composition of skeletal musculature of the forelimb in young and aged wild type and myostatin null mice. Rejuvenation Res. 12: 269–281. https://doi.org/10.1089/rej.2009.0870

Elkasrawy, M. N., and M. W. Hamrick, 2010 Myostatin (GDF-8) as a key factor linking muscle mass and bone structure. J. Musculoskelet. Neuronal Interact. 10: 56–63.

Gesualdi, S. C., and T. E. Haerry, 2007 Distinct signaling of *Drosophila* Activin/TGF-beta family members. Fly (Austin) 1: 212–221. https://doi.org/10.4161/fly.5116

Ghosh, A. C., and M. B. O'Connor, 2014 Systemic activin signaling independently regulates sugar homeostasis, cellular metabolism, and pH balance in *Drosophila* melanogaster. Proc. Natl. Acad. Sci. USA 111: 5729–5734. https://doi.org/10.1073/pnas.1319116111

Gibbens, Y. Y., J. T. Warren, L. I. Gilbert, and M. B. O'Connor, 2011 Neuroendocrine regulation of Drosophila metamorphosis requires TGFbeta/Activin signaling. Development 138: 2693–2703. https://doi.org/10.1242/dev.063412

Goberdhan, D. C., N. Paricio, E. C. Goodman, M. Mlodzik, and C. Wilson, 1999 *Drosophila* tumor suppressor PTEN controls cell size and number by antagonizing the Chico/PI3-kinase signaling pathway. Genes Dev. 13: 3244–3258. https://doi.org/10.1101/gad.13.24.3244

Gokhale, R. H., T. Hayashi, C. D. Mirque, and A. W. Shingleton, 2016 Intra-organ growth coordination in *Drosophila* is mediated by systemic ecdysone signaling. Dev. Biol. 418: 135–145. https://doi.org/10.1016/j.ydbio.2016.07.016

Hariharan, I. K., D. B. Wake, and M. H. Wake, 2015 Indeterminate growth: could it represent the ancestral condition? Cold Spring Harb. Perspect. Biol. 8: a019174. https://doi.org/10.1101/cshperspect.a019174

Hata, A., and Y. G. Chen, 2016 TGF-β signaling from receptors to Smads. Cold Spring Harb. Perspect. Biol. 8: a022061. https://doi.org/10.1101/cshperspect.a022061

Heldin, C. H., and A. Moustakas, 2016 Signaling receptors for TGF-β family members. Cold Spring Harb. Perspect. Biol. 8: a022053. https://doi.org/10.1101/cshperspect.a022053

Hill, C. S., 2016 Transcriptional control by the SMADs. Cold Spring Harb. Perspect. Biol. 8: a022079. https://doi.org/10.1101/cshperspect.a022079

Hirschhorn, J. N., and G. Lettre, 2009 Progress in genome-wide association studies of human height. Horm. Res. 71: 5–13.

Jensen, P. A., X. Zheng, T. Lee, and M. B. O'Connor, 2009 The *Drosophila* Activin-like ligand Dawdle signals preferentially through one isoform of the Type-I receptor Baboon. Mech. Dev. 126: 950–957. https://doi.org/10.1016/j.mod.2009.09.003

Kahlem, P., and S. J. Newfeld, 2009 Informatics approaches to understanding TGFbeta pathway regulation. Development 136: 3729–3740. https://doi.org/10.1242/dev.030320

Kim, M. J., and M. B. O'Connor, 2014 Anterograde Activin signaling regulates postsynaptic membrane potential and GluRIIA/B abundance at the *Drosophila* neuromuscular junction. PLoS One 9: e107443. https://doi.org/10.1371/journal.pone.0107443

Koyama, T., and C. K. Mirth, 2018 Unravelling the diversity of mechanisms through which nutrition regulates body size in insects. Curr. Opin. Insect Sci. 25: 1–8. https://doi.org/10.1016/j.cois.2017.11.002

Kronenberg, H. M., 2003 Developmental regulation of the growth plate. Nature 423: 332–336. https://doi.org/10.1038/nature01657

Lamouille, S., and R. Derynck, 2007 Cell size and invasion in TGF-beta-induced epithelial to mesenchymal transition is regulated by activation of the mTOR pathway. J. Cell Biol. 178: 437–451. https://doi.org/10.1083/jcb.200611146

Lee, G., and J.H. Park, 2004 Hemolymph sugar homeostasis and starvation-induced hyperactivity affected by genetic manipulations of the adipokinetic hormone-encoding gene in *Drosophila melanogaster*. Genetics 167: 311–323. https://doi.org/10.1534/genetics.167.1.311

Lee, J. Y., N. S. Hopkinson, and P. R. Kemp, 2011 Myostatin induces autophagy in skeletal muscle in vitro. Biochem. Biophys. Res. Commun. 415: 632–636. https://doi.org/10.1016/j.bbrc.2011.10.124

Leevers, S. J., D. Weinkove, L. K. MacDougall, E. Hafen, and M. D. Waterfield, 1996 The *Drosophila* phosphoinositide 3-kinase Dp110 promotes cell growth. EMBO J. 15: 6584–6594. https://doi.org/10.1002/j.1460-2075.1996.tb01049.x

Lokireddy, S., I. W. Wijesoma, S. K. Sze, C. McFarlane, R. Kambadur *et al.*, 2012 Identification of atrogin-1-targeted proteins during the myostatin-induced skeletal muscle wasting. Am. J. Physiol. Cell Physiol. 303: C512–C529. https://doi.org/10.1152/ajpcell.00402.2011

Macias, M. J., P. Martin-Malpartida, and J. Massague, 2015 Structural determinants of Smad function in TGF-beta signaling. Trends Biochem. Sci. 40: 296–308. https://doi.org/10.1016/j.tibs.2015.03.012

Madaan, U., E. Yzeiraj, M. Meade, J. F. Clark, C. A. Rushlow *et al.*, 2018 BMP signaling determines body size via transcriptional regulation of collagen genes in Caenorhabditis elegans. Genetics 210: 1355–1367. https://doi.org/10.1534/genetics.118.301631

Makhijani, K., B. Alexander, D. Rao, S. Petraki, L. Herboso *et al.*, 2017 Regulation of *Drosophila* hematopoietic sites by Activin-beta from active sensory neurons. Nat. Commun. 8: 15990. https://doi.org/10.1038/ncomms15990

Marqués, G., H. Bao, T. E. Haerry, M. J. Shimell, P. Duchek *et al.*, 2002 The *Drosophila* BMP type II receptor Wishful Thinking regulates neuromuscular synapse morphology and function. Neuron 33: 529–543. https://doi.org/10.1016/S0896-6273(02)00595-0

Matsakas, A., A. Otto, M. I. Elashry, S. C. Brown, and K. Patel, 2010 Altered primary and secondary myogenesis in the myostatin-null mouse. Rejuvenation Res. 13: 717–727. https://doi.org/10.1089/rej.2010.1065

McBrayer, Z., H. Ono, M. Shimell, J. P. Parvy, R. B. Beckstead *et al.*, 2007 Prothoracicotropic hormone regulates developmental timing and body size in *Drosophila*. Dev. Cell 13: 857–871. https://doi.org/10.1016/j.devcel.2007.11.003

McNabb, S. L., J. D. Baker, J. Agapite, H. Steller, L. M. Riddiford *et al.*, 1997 Disruption of a behavioral sequence by targeted death of peptidergic neurons in *Drosophila*. Neuron 19: 813–823. https://doi.org/10.1016/S0896-6273(00)80963-0

McPherron, A. C., and S. J. Lee, 1997 Double muscling in cattle due to mutations in the myostatin gene. Proc. Natl. Acad. Sci. USA 94: 12457–12461. https://doi.org/10.1073/pnas.94.23.12457

McPherron, A. C., A. M. Lawler, and S. J. Lee, 1997 Regulation of skeletal muscle mass in mice by a new TGF-beta superfamily member. Nature 387: 83–90. https://doi.org/10.1038/387083a0

Mirth, C. K., and A. W. Shingleton, 2012 Integrating body and organ size in *Drosophila*: recent advances and outstanding problems. Front. Endocrinol. (Lausanne) 3: 49. https://doi.org/10.3389/fendo.2012.00049

Mirth, C. K., and A. W. Shingleton, 2014 The roles of juvenile hormone, insulin/target of rapamycin, and ecdysone signaling in regulating body size in *Drosophila*. Commun. Integr. Biol. 7: e971568. https://doi.org/10.4161/cib.29240

Mirth, C. K., H. Y. Tang, S. C. Makohon-Moore, S. Salhadar, R. H. Gokhale *et al.*, 2014 Juvenile hormone regulates body size and perturbs insulin signaling in *Drosophila*. Proc. Natl. Acad. Sci. USA 111: 7018–7023. https://doi.org/10.1073/pnas.1313058111

Nijhout, H. F., and V. Callier, 2015 Developmental mechanisms of body size and wing-body scaling in insects. Annu. Rev. Entomol. 60: 141–156. https://doi.org/10.1146/annurev-ento-010814-020841

Nijhout, H. F., and L. W. Grunert, 2010 The cellular and physiological mechanism of wing-body scaling in Manduca sexta. Science 330: 1693–1695. https://doi.org/10.1126/science.1197292

Oldham, S., J. Montagne, T. Radimerski, G. Thomas, and E. Hafen, 2000 Genetic and biochemical characterization of dTOR, the *Drosophila* homolog of the target of rapamycin. Genes Dev. 14: 2689–2694. https://doi.org/10.1101/gad.845700

Park, D., J. A. Veenstra, J. H. Park, and P. H. Taghert, 2008 Mapping peptidergic cells in *Drosophila*: where DIMM fits in. PLoS One 3: e1896. https://doi.org/10.1371/journal.pone.0001896

Parker, N. F., and A. W. Shingleton, 2011 The coordination of growth among *Drosophila* organs in response to localized growth-perturbation. Dev. Biol. 357: 318–325. https://doi.org/10.1016/j.ydbio.2011.07.002

Prokop, A., 2006 Organization of the efferent system and structure of neuromuscular junctions in *Drosophila*. Int. Rev. Neurobiol. 75: 71–90. https://doi.org/10.1016/S0074-7742(06)75004-8

Prokop, A., and I. A. Meinertzhagen, 2006 Development and structure of synaptic contacts in *Drosophila*. Semin. Cell Dev. Biol. 17: 20–30. https://doi.org/10.1016/j.semcdb.2005.11.010

Ren, X., J. Sun, B. E. Housden, Y. Hu, C. Roesel *et al.*, 2013 Optimized gene editing technology for *Drosophila* melanogaster using germ line-specific Cas9. Proc. Natl. Acad. Sci. USA 110: 19012–19017. https://doi.org/10.1073/pnas.1318481110

Rewitz, K. F., N. Yamanaka, L. I. Gilbert, and M. B. O'Connor, 2009 The insect neuropeptide PTTH activates receptor tyrosine kinase torso to initiate metamorphosis. Science 326: 1403–1405. https://doi.org/10.1126/science.1176450

Rewitz, K. F., N. Yamanaka, and M. B. O'Connor, 2013 Developmental checkpoints and feedback circuits time insect maturation. Curr. Top. Dev. Biol. 103: 1–33. https://doi.org/10.1016/B978-0-12-385979-2.00001-0

Riddiford, L. M., J. W. Truman, C. K. Mirth, and Y. C. Shen, 2010 A role for juvenile hormone in the prepupal development of *Drosophila* melanogaster. Development 137: 1117–1126. https://doi.org/10.1242/dev.037218

Rulifson, E. J., S. K. Kim, and R. Nusse, 2002 Ablation of insulin-producing neurons in flies: growth and diabetic phenotypes. Science 296: 1118–1120. https://doi.org/10.1126/science.1070058

Sartori, R., E. Schirwis, B. Blaauw, S. Bortolanza, J. Zhao *et al.*, 2013 BMP signaling controls muscle mass. Nat. Genet. 45: 1309–1318. https://doi.org/10.1038/ng.2772

Schindelin, J., I. Arganda-Carreras, E. Frise, V. Kaynig, M. Longair *et al.*, 2012 Fiji: an open-source platform for biological-image analysis. Nat. Methods 9: 676–682. https://doi.org/10.1038/nmeth.2019

Sebo, Z. L., H. B. Lee, Y. Peng, and Y. Guo, 2014 A simplified and efficient germline-specific CRISPR/Cas9 system for *Drosophila* genomic engineering. Fly (Austin) 8: 52–57. https://doi.org/10.4161/fly.26828

Shim, K. S., 2015 Pubertal growth and epiphyseal fusion. Ann. Pediatr. Endocrinol. Metab. 20: 8–12. https://doi.org/10.6065/apem.2015.20.1.8

Shimell, M., X. Pan, F. A. Martin, A. C. Ghosh, P. Leopold *et al.*, 2018 Prothoracicotropic hormone modulates environmental adaptive plasticity through the control of developmental timing. Development 145: dev159699. https://doi.org/10.1242/dev.159699

Shingleton, A. W., and W. A. Frankino, 2013 New perspectives on the evolution of exaggerated traits. Bioessays 35: 100–107. https://doi.org/10.1002/bies.201200139

Shingleton, A. W., W. A. Frankino, T. Flatt, H. F. Nijhout, and D. J. Emlen, 2007 Size and shape: the developmental regulation of static allometry in insects. Bioessays 29: 536–548. https://doi.org/10.1002/bies.20584

Shingleton, A. W., C. M. Estep, M. V. Driscoll, and I. Dworkin, 2009 Many ways to be small: different environmental regulators of size generate distinct scaling relationships in *Drosophila* melanogaster. Proc. Biol. Sci. 276: 2625–2633. https://doi.org/10.1098/rspb.2008.1796

Siegmund, T., and G. Korge, 2001 Innervation of the ring gland of *Drosophila* melanogaster. J. Comp. Neurol. 431: 481–491. https://doi.org/10.1002/1096-9861(20010319)431:4<481::AID-CNE1084>3.0.CO;2-7

Simpson, P., and H. A. Schneiderman, 1975 Isolation of temperature sensitive mutations blocking clone development in Drosophila melanogaster, and the effects of a temperature sensitive cell lethal mutation on pattern formation in imaginal discs. Wilehm. Roux. Arch. Dev. Biol. 178: 247–275. https://doi.org/10.1007/BF00848432

Simpson, P., P. Berreur, and J. Berreur-Bonnenfant, 1980 The initiation of pupariation in *Drosophila*: dependence on growth of the imaginal discs. J. Embryol. Exp. Morphol. 57: 155–165.

Song, W., D. Cheng, S. Hong, B. Sappe, Y. Hu *et al.*, 2017a Midgut-derived activin regulates glucagon-like action in the fat body and glycemic control. Cell Metab. 25: 386–399. https://doi.org/10.1016/j.cmet.2017.01.002

Song, W., E. Owusu-Ansah, Y. Hu, D. Cheng, X. Ni *et al.*, 2017b Activin signaling mediates muscle-to-adipose communication in a mitochondria dysfunction-associated obesity model. Proc. Natl. Acad. Sci. USA. 114: 8596–8601. https://doi.org/10.1073/pnas.1708037114

Stieper, B. C., M. Kupershtok, M. V. Driscoll, and A. W. Shingleton, 2008 Imaginal discs regulate developmental timing in *Drosophila* melanogaster. Dev. Biol. 321: 18–26. https://doi.org/10.1016/j.ydbio.2008.05.556

Stocker, H., T. Radimerski, B. Schindelholz, F. Wittwer, P. Belawat *et al.*, 2003 Rheb is an essential regulator of S6K in controlling cell growth in *Drosophila*. Nat. Cell Biol. 5: 559–565. https://doi.org/10.1038/ncb995

Ting, C. Y., T. Herman, S. Yonekura, S. Gao, J. Wang *et al.*, 2007 Tiling of r7 axons in the *Drosophila* visual system is mediated both by transduction of an activin signal to the nucleus and by mutual repulsion. Neuron 56: 793–806. https://doi.org/10.1016/j.neuron.2007.09.033

Ting, C. Y., P. G. McQueen, N. Pandya, T. Y. Lin, M. Yang *et al.*, 2014 Photoreceptor-derived activin promotes dendritic termination and restricts the receptive fields of first-order interneurons in *Drosophila*. Neuron 81: 830–846. https://doi.org/10.1016/j.neuron.2013.12.012

Trendelenburg, A. U., A. Meyer, D. Rohner, J. Boyle, S. Hatakeyama *et al.*, 2009 Myostatin reduces Akt/TORC1/p70S6K signaling, inhibiting myoblast differentiation and myotube size. Am. J. Physiol. Cell Physiol. 296: C1258–C1270. https://doi.org/10.1152/ajpcell.00105.2009

Tuck, S., 2014 The control of cell growth and body size in Caenorhabditis elegans. Exp. Cell Res. 321: 71–76. https://doi.org/10.1016/j.yexcr.2013.11.007

Upadhyay, A., L. Moss-Taylor, M. J. Kim, A. C. Ghosh, and M. B. O'Connor, 2017 TGF-β family signaling in *Drosophila*. Cold Spring Harb. Perspect. Biol. 9: a022152.

Winbanks, C. E., J. L. Chen, H. Qian, Y. Liu, B. C. Bernardo *et al.*, 2013 The bone morphogenetic protein axis is a positive regulator of skeletal muscle mass. J. Cell Biol. 203: 345–357. https://doi.org/10.1083/jcb.201211134

Wood, A. R., T. Esko, J. Yang, S. Vedantam, T. H. Pers *et al.*, 2014 Defining the role of common variation in the genomic and biological architecture of adult human height. Nat. Genet. 46: 1173–1186. https://doi.org/10.1038/ng.3097

Wu, Q., T. Wen, G. Lee, J. H. Park, H. N. Cai *et al.*, 2003 Developmental control of foraging and social behavior by the *Drosophila* neuropeptide Y-like system. Neuron 39: 147–161. https://doi.org/10.1016/S0896-6273(03)00396-9

Wu, Q., Y. Zhang, J. Xu, and P. Shen, 2005 Regulation of hunger-driven behaviors by neural ribosomal S6 kinase in *Drosophila*. Proc. Natl. Acad. Sci. USA 102: 13289–13294. https://doi.org/10.1073/pnas.0501914102

Yamanaka, N., K. F. Rewitz, and M. B. O'Connor, 2013a Ecdysone control of developmental transitions: lessons from *Drosophila* research. Annu. Rev. Entomol. 58: 497–516. https://doi.org/10.1146/annurev-ento-120811-153608

Yamanaka, N., N. M. Romero, F. A. Martin, K. F. Rewitz, M. Sun *et al.*, 2013b Neuroendocrine control of *Drosophila* larval light preference. Science 341: 1113–1116. https://doi.org/10.1126/science.1241210

Zhou, X., J. L. Wang, J. Lu, Y. Song, K. S. Kwak *et al.*, 2010 Reversal of cancer cachexia and muscle wasting by ActRIIB antagonism leads to prolonged survival. Cell 142: 531–543. https://doi.org/10.1016/j.cell.2010.07.011

Zhu, C. C., J. Q. Boone, P. A. Jensen, S. Hanna, L. Podemski *et al.*, 2008 *Drosophila* Activin- and the Activin-like product Dawdle function redundantly to regulate proliferation in the larval brain. Development 135: 513–521. https://doi.org/10.1242/dev.010876

Communicating editor: D. Andrew